Spectrochimica Acta Part B: Atomic Spectroscopy 199 (2023) 106570

Contents lists available at ScienceDirect

Spectrochimica Acta Part B: Atomic Spectroscopy

journal homepage: www.elsevier.com/locate/sab

Invited review

Catching particles by atomic spectrometry: Benefits and limitations of single particle - inductively coupled plasma mass spectrometry

Francisco Laborda *, Isabel Abad-Álvaro, María S. Jiménez, Eduardo Bolea

Group of Analytical Spectroscopy and Sensors (GEAS), Institute of Environmental Sciences (IUCA), Universidad de Zaragoza, Pedro Cerbuna 12, 50009 Zaragoza, Spain

ARTICLE INFO

Keywords:
Single particle detection
ICP-MS
Fundamentals
Nanoparticles
Microparticles

ABSTRACT

Single particle inductively coupled plasma mass spectrometry (SP-ICP-MS) has led ICP-MS into a new dimension, turning an ensemble technique for elemental and isotope ratio analysis into a particle counting technique and well beyond. SP-ICP-MS allows the detection of particles, their size characterization and the quantification of their number and mass concentrations, as well as the dissolved forms of the target element(s). Although the technique is mostly applied to metal- and metalloid-based nanoparticles, its application to microparticles and carbon-based particles are emerging. After twenty years since the first publications and more than ten years of ongoing development, SP-ICP-MS has reached a high degree of maturity, with an increasing number of applications in a wide range of fields. Despite this trend, there are aspects related to the fundamentals of the technique that still require further studies. This review is organized around the fundamentals of the technique along with the different steps and processes involved, from the sample introduction to the signal processing, offering an updated view of these topics, focusing on the benefits and current limitations of the technique, as well as its future perspectives.

1. Introduction

The relevance of nanomaterials and nanoparticles has attracted attention from all scientific fields, and analytical chemistry and spectroscopy are no exception. In this case, nanoparticles have emerged as a new type of analytes with very particular features due to their physicochemical nature. Whereas for conventional analytes, the information demanded can be quantitative (e.g., mass concentration), as well as qualitative (including the identification of the chemical species), the situation is more complex for nanoparticles: the quantitative information can be demanded as mass but also as number concentration, and the qualitative information can involve not just the detection of the nanoparticle as such, but also include both chemical and physical characterization (e.g. size, shape, aggregation/agglomeration) [1]. Atomic spectrometry in general and particularly inductively coupled plasma mass spectrometry (ICP-MS) were not expected to have a relevant role in the analysis of nanomaterials or samples containing nanoparticles, other than providing element compositions and element mass concentrations, or being used as element specific detectors coupled to nanoparticle separation techniques (e.g., flow field flow fractionation, hydrodynamic chromatography). However, ICP-MS was able to reinvent itself as a particle counting technique, just by using very high data acquisition frequencies for measuring suspensions of nanoparticles sufficiently diluted. Under such conditions, ICP-MS is able to provide information on a particle-by-particle basis, giving rise to the so-called single particle ICP-MS (SP-ICP-MS) [2].

Handling particles is not new in ICP-MS. Although different approaches have been developed for the introduction of powdered samples into plasmas (e.g., fluidized bed chambers, direct sample injection devices, electrothermal vaporization), slurry nebulization is the approach that has received major consideration in the field [3]. The main difference between the analysis of solid samples by slurry nebulization and the analysis of samples containing nanoparticles is that in slurry nebulization the suspensions of particles are prepared ad-hoc, by grinding the solid sample to particles of the adequate size (in the micrometer range) and dispersing them into the adequate liquid medium at the adequate particle concentration. When analyzing samples originally containing particles, we might just modify their concentration because the analyte is the particles themselves instead of the element/s present in the particles. In spite of these differences, some of the strategies followed for the analysis of powdered solids by slurry nebulization can be useful in SP-ICP-MS. In a similar way, Poisson statistics are at the core of ICP-MS

* Corresponding author.
E-mail address: flaborda@unizar.es (F. Laborda).

https://doi.org/10.1016/j.sab.2022.106570
Received 23 May 2022; Received in revised form 9 November 2022; Accepted 9 November 2022
Available online 13 November 2022

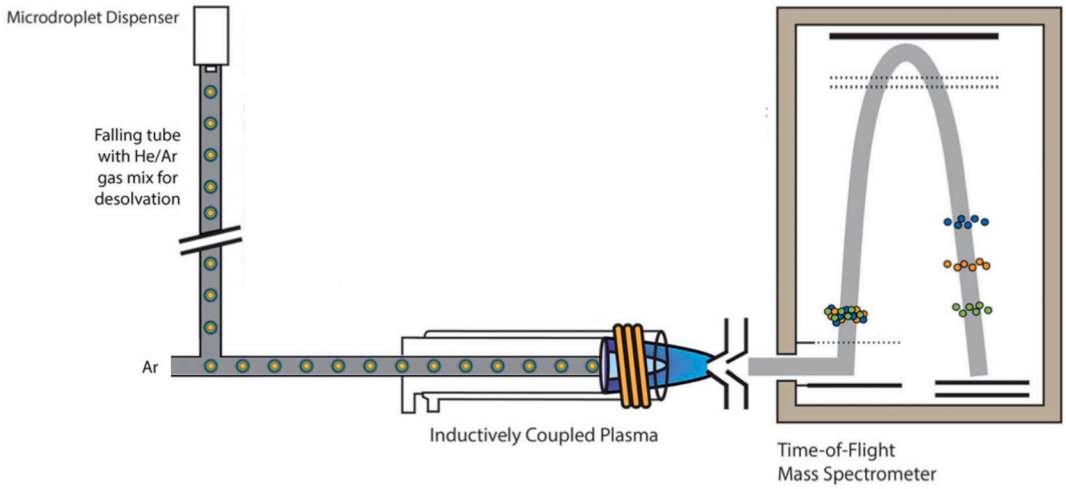

Fig. 1. Schematic diagram of a microdroplet generator for sample introduction in an ICP-TOF-MS instrument. Adapted from [30] with permission from the Royal Chemical Society.

in relation with ion counting; however, SP-ICP-MS, as both ion and particle counting technique, has had to revisit Poisson approaches [4] to deal with data processing [5], metrology [6] and modelling [7,8].

The basics and applications of SP-ICP-MS have been shown and summarized in several reviews [6,9–14] and they will not be discussed here. SP-ICP-MS is gaining recognition as a mature technique because their methods are being applied to a wide range of analytical problems and determinations, and it is becoming established as a routine tool with broad commercialization. This maturity is reflected in the increasing number of publications related to applications, whereas those related to the basics of the technique and the development of methods are fewer and not growing [13]. Despite this trend, the fundamentals of the technique are far from being completely developed and there is still room for further studies and discussion. The aim of this review is to focus on the fundamental aspects of the technique along with the different steps and processes involved, from the sample introduction to the signal processing, showing the limitations and benefits of the technique, as well as its future perspectives.

2. Sample introduction

Most of the work in SP-ICP-MS involves working with nanoparticle suspensions, which are introduced into the instruments as liquid aerosols by nebulization. However, in recent years, laser ablation, a well-stablished method for the introduction of solid samples in ICP-MS has been adapted to deal with nanoparticles. Both sample introduction approaches will be discussed in the context of SP-ICP-MS.

2.1. Nebulization

Nanoparticles, defined as nano-objects with their three external dimensions in the range of 1–100 nm, behave like dissolved species from the point of view of their nebulization. Typical nebulization systems consist of pneumatic nebulizers in combination with spray chambers with reported transport efficiencies in the range of 1–10% by applying sample flow rates of 0.1–1 mL min^{-1}. In this review transport efficiency is a synonymous of nebulization efficiency, being only related to the sample introduction process up to the plasma.

The relevance of the transport efficiency in SP-ICP-MS lies in the fact that, together with the sample flow rate, is a parameter required for calculation of the mass of element per particle, and hence the size of the particles (if their composition, shape and density are known), when using the calibration with dissolved standards of the monitored element. This size calibration approach is an alternative to the use of size standards of the particles analyzed, as it will be also discussed in the next section. The determination of analyte transport efficiency in atomic spectrometry has been traditionally performed by using direct (aerosol collection) and indirect (waste collection) methods with dissolved standards [15], although the use of nanoparticle standards has allowed the development of alternative methods, namely the frequency and the size methods [16]. More recently, a dynamic mass flow (DMF) method has been proposed [17]. Although the DMF method does not rely on the use of any analyte standard, the transport efficiency determined corresponds to the solvent transport, which can be equated with the analyte transport under conditions that make the solvent vaporization negligible [18]. On the other hand, the frequency method requires number concentration standards of an easily detectable nanoparticle, which has just become available recently [19], or, alternatively, size standards of monodispersed metallic nanoparticles with known metal mass concentration. Finally, the size method is based on the use of nanoparticle size standards as well as dissolved standards of the element present in the nanoparticles, assuming that the element, both in the nanoparticle and dissolved standards, behave in the same way in the plasma, which is not always the case. Details about the procedures and calculations of transport efficiencies by these methods can be found elsewhere [16,17]. The three methods have been evaluated through an interlaboratory comparison study [18].

In view of so many conditioning factors, the use of high throughput sample introduction systems with 100% of transport efficiency has been proposed to remove this source of uncertainty in SP-ICP-MS. Nowadays, 100% transport efficiencies can be achieved by using direct injection nebulization or microdroplet generation (MDG).

Microdroplet generation was firstly applied for sample introduction to plasmas in optical emission spectrometry [20–22], being further adapted to ICP-MS [23]. Microdroplet generators used in SP-ICP-MS are based on a dispenser head consisting of a piezoelectrically actuated quartz capillary that delivers discrete well-defined volumes of liquids as individual droplets of 25–50 μm at a frequency of 100 Hz [24]. The droplets are carried by a flow of helium, being desolvated in their way to the plasma and producing dry particles that further contributes to improve transport efficiency up to practically 100%, as well as their vaporization and ionization [25]. Finally, matrix effects caused by high salt or organic contents are limited as a result of the low sample uptake used (50–400 nL min^{-1}). An additional advantage of MDG is that calibration can be performed with dissolved standards because the amount of element per droplet can be known due to the low dispersion of the droplet diameters. MDG has been evaluated in combination with quadrupole [23], double focusing [25,26] and time-of-flight instruments

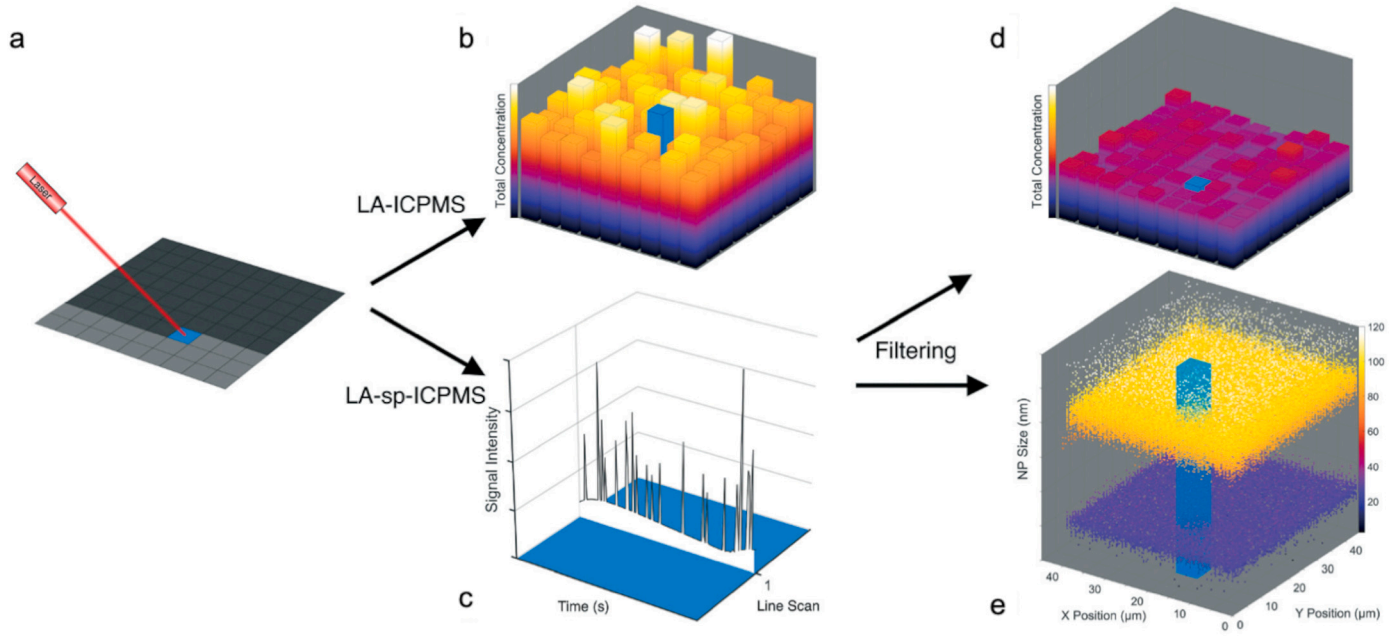

Fig. 2. Comparison of conventional LA-ICP-MS (low time resolution) and multimodal LA-SP-ICP-MS (high time resolution) mapping upon simulated laser ablation of a sample containing homogeneously distributed Ag^+ and Ag nanoparticles. (a) Laser ablation line scanning; (b) total silver surface distribution map; (c) raw high time resolution data for one pixel; (d) Ag^+ surface distribution map; (e) combined Ag nanoparticle surface distribution and size map. The light blue squares and columns show the information contained in a single pixel [51]. With permission from the Royal Society of Chemistry. *(For interpretation of the references to colour in this figure legend, the reader is referred to the web version of this article.)*

[27–29]. A schematic diagram of the setup coupled to a time-of-flight instrument is shown in Fig. 1.

The second option to obtain 100% analyte transport efficiency is the use of direct injection devices, working with micro-flows below 10 μL min^{-1} and removing the spray chamber [31,32]. Tharaud et al. [32] have reported a micro-flow sample introduction system consisting of a demountable direct injection high-efficiency nebulizer (dDIHEN) hyphenated to a flow-injection valve and a gas displacement pump. Alternatively, nebulization setups consisting of micro-flow nebulizer and specially designed spray chamber have been reported. Sun et al. [33] achieved transport efficiencies over 90% at 5 μL min^{-1} by using an in-house cyclonic spray chamber without baffle. Miyashita et al., by using a setup consisting of a high performance concentric nebulizer and a custom-made small-volume on-axis spray chamber equipped with an additional sheath gas [34], reported transport efficiencies of 93% at 8.6 μL min^{-1} [35] and 99% at 9.8 μL min^{-1} [36]. The same nebulizer was used in combination with an APEX system, consisting of a heated cyclonic spray chamber (140 °C) and a three-stage Peltier-cooled desolvation system (2 °C), reporting a 104% transport efficiency at 10-times higher flow rates of 103 μL min^{-1} [36].

The basic assumption behind SP-ICP-MS is that each particle event recorded is produced by a single particle, which requires the use of suspensions sufficiently diluted so that the flux of particles reaching the plasma is sufficiently low (<100 s^{-1}) [37]. Under such conditions, some aerosol droplets will contain one particle and most of them none. Whereas the transport of aerosol droplets with diameters of tens of micrometers is not affected by the presence of a particle of nanometers, this might not be the case when the size of the particles is also in the micrometer range. Fundamental studies with slurries have shown that nebulization and transport of microparticles is affected by their size and density, as well as the nebulization system used, although in general terms transport efficiency for particles over 5–20 μm drops significantly and particles in the upper end may even not reach the plasma [38]. The single particle occupancy (SPO) model, developed by Goodall et al. [39] allows estimating a maximum allowable particle diameter (the single occupancy diameter) for which every single droplet of the aerosol contains one solid particle, at a specific slurry concentration. Under such conditions, the density of particle-loaded aerosol droplets do not deviate appreciably from that of vacant aerosol droplets, and the presence of a solid particle within an aerosol droplet does not modify itself the transport behavior of the original aerosol. They predicted maximum diameters from 3 to 1.5 μm for particles with densities from 1 to 7 g mL^{-1} and a slurry concentration of 1% (m/v), for a specific nebulization setup [39]. The experience from slurry nebulization and other recent studies [40,41], suggest that number concentration determinations involving microparticles can be severely biased in SP-ICP-MS otherwise the effect of the size of the particles on their transport is considered. This is a matter of concern in single cell ICP-MS, where soft bioparticles in the micrometer range must be nebulized as intact entities [42].

2.2. Laser ablation

Laser ablation (LA) is widely used as solid sample introduction technique for ICP-MS, being LA-ICP-MS a well-established technique for quantitative elemental analysis and mapping [43]. LA is inherently based on the formation of aerosols of nano and micrometer sized particles upon laser exposure of the sample [44]. Donard et al. [45] determined the particle size distribution of aerosols produced by femtosecond lasers using a methodology based on SP-ICP-MS, confirming that particles larger than 159 nm represented <1% of the aerosol whole distribution. However, the application of LA to the analysis of samples originally containing nanoparticles requires a different approach not solely based on the increase of the time resolution, as it is summarized in Fig. 2. Until now, the use of LA as sample introduction technique in combination with SP-ICP-MS has allowed the direct analysis of solid materials containing nanoparticles [46] as well as particulate materials [47], avoiding the extraction of nanoparticles to liquid phases, but also adding spatial resolution and imaging features [48–51].

Laser ablation was firstly used in combination with SP-ICP-MS as substrate-assisted laser desorption (SALD) [52], being applied to the direct analysis of gold nanoparticles from dried droplets deposited on polyethylene terephthalate glycol (PETG) plates. Desorption of

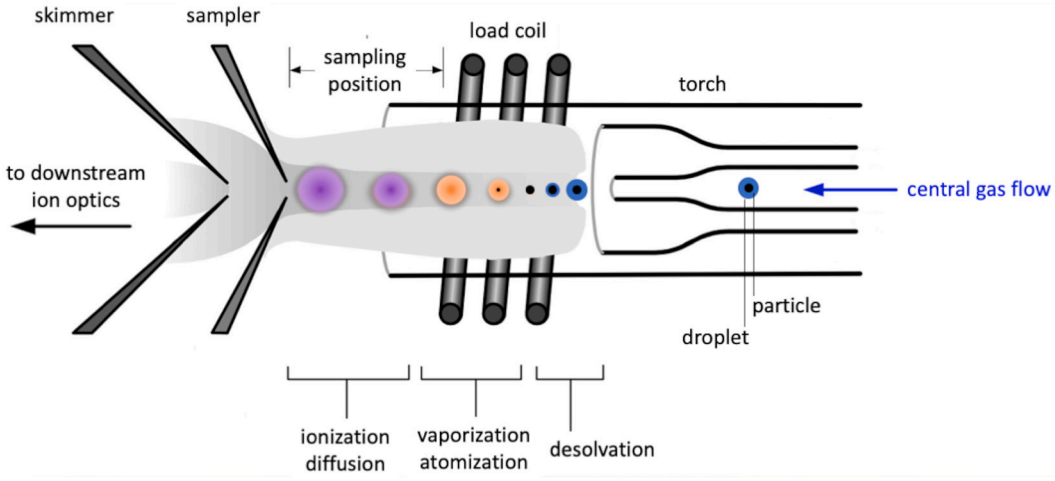

Fig. 3. Processes from particle in a droplet to ions detected by SP-ICP-MS. (Particle, droplet and ion cloud are not drawn to scale). Adapted from [10] with permission from Springer Nature.

individual gold nanoparticles by SALD was based on the use of a Nd:YAG laser operated at low laser fluence (<1 J cm^{-2}). A 100 μm diameter laser beam spot, at 20 Hz frequency and 200 μm s^{-1} scan rate were selected as optimum scanning conditions to irradiate the whole spot of a droplet dry residue and desorbing the Au nanoparticles. Helium provided better results than argon as carrier gas, achieving transport efficiencies of 61% for nanoparticles.

The use of low fluences (0.1–1 J cm^{-2}) to avoid the degradation of the particles is reported in most publications regarding LA-SP-ICP-MS [46,48–54]. Metarapi et al. [50,53], by using custom-made gelatin standards doped with Au nanoparticles, confirmed the requirement of low fluences for releasing the nanoparticles from the matrix, minimizing their degradation and retrieving the correct mean particle size. They showed that higher fluences not only led to an increase in the total number of nanoparticles detected but also in smaller ones, distorting the original size distributions. The use of the lowest laser fluence the sample ablation threshold allowed was recommended. However, even under low fluence conditions the authors also reported a significant broadening of the size distributions measured by LA-SP-ICP-MS in comparison with the manufacturer data, which they considered to arise due to Poisson noise [53].

The type of laser also influences the size distribution of nanoparticles measured by LA-SP-ICP-MS. Yamashita et al. [49] studied the effect of femto- and nanosecond lasers on Au and Ag nanoparticles. They observed that femtosecond lasers produced broader size distributions, with an increase of smaller nanoparticles, suggesting a significant degradation of the original nanoparticles due to the higher ablation efficiencies of femtosecond laser for metallic materials and recommending the use of nanosecond lasers for obtaining reliable size distributions.

In a similar way that the dissolved element in a suspension contributes to increase the intensity of the continuous baseline in nebulization SP-ICP-MS, the presence of non-particulate element in the solid matrix leads upon ablation to the generation of matrix-related particles containing low amounts of the target element, producing low intensity spikes with a width of 50–500 ms per LA pulse, which lead to a continuous signal, as in conventional LA-ICP-MS, as it can be seen in Fig. 2.

Tuoriniemi et al. [46] proposed to couple the plasma torch via a T-section to both the laser ablation and the nebulization systems for matrix matching of the calibration standards by simultaneously ablating a control solid matrix (a non-spiked soil). By using this arrangement, the authors demonstrated that size and number concentration of Au nanoparticles in soils were determined accurately by following the same calibration procedure than for nebulization SP-ICP-MS, by using dissolved standards and size-certified particles.

By combining laser ablation with a time-of-flight instrument (LA-SP-ICP-TOF-MS), Holbrook et al. [47] investigated the direct analysis of multi-elemental particles in sediments. When compared with the analysis of the particles isolated by cloud point extraction and nebulizer SP-ICP-TOF-MS, both methods produced comparable results for elemental ratios and single-particle fingerprinting. However, LA-SP-ICP-TOF-MS revealed a more complex picture of the composition of the multi-elemental particles, detecting more complex single and aggregated particle distributions for rare earth and platinum group elements.

3. Plasma processes

Once a particle reaches the plasma, previously desolvated if in an aerosol droplet, the particle must be volatilized/atomized and their atoms ionized to produce a cloud of ions that will be sampled through the interface into the mass spectrometer. All these processes (Fig. 3) take place during the residence time of the particles in the plasma, which depends on the central gas flow rate, the inner diameter of the injector, the sampling position and the power used to generate the plasma [55].

Before the emergence of SP-ICP-MS, fundamental studies about plasma processes by considering individual droplets and particles had been carried out both experimental and computationally. These studies were pioneered by Olesik [20] and have been summarized in [56]. Those interested in these fundamental studies can refer to the references therein, since we will only focus here on those aspects that are most relevant in the context of SP-ICP-MS.

The intensity of the signal produced by a single particle does not depend on its nebulization, but on its degree of volatilization/atomization/ionization in combination with the diffusion of the ions in the plasma [57] and their subsequent extraction through the interface. Focusing on the volatilization, atomization and ionization processes, the efficiency of these processes depends on the particle properties (size, density, composition, boiling point of its component/s), the ionization potential of the monitored element and the ICP operating parameters (ICP forward power, injector inner diameter and central channel gas flow rate) [57], whereas diffusion depends on isotope mass and the time that the ions spend in the plasma prior to extraction [55].

Fuchs et al. [58] modeled the behavior of Au nanoparticles in the plasma with respect to their size. They showed that the extent of the ion cloud depends on the particle diameter, in agreement with the experimental data, ranging from 300 μs for 15 nm up to 1000 μs for 80 nm under the conditions tested. Whereas the Au^{+} number density for the different particle diameters showed the maxima at the same point along

the central axis of the plasma, it remained at higher levels over a longer distance downstream for larger particles, increasing the duration of the recorded particle events. The summed-up intensity of the particle events was proportional to the Au mass in the size range studied, which was not the case for larger particles due to their incomplete volatilization using the selected plasma conditions. In line with these studies, Ho et al. [57] developed a mathematical model to calculate the degree of particle vaporization, which predicts that larger particles with low boiling points, densities and molecular masses are more easily volatilized. Whereas the boiling point of the particle determines the starting position of vaporization in the plasma, the vaporization rate depends on its molecular mass and density. Considering all these factors in combination with the residence time of the particles in the plasma and selecting a specific set of plasma conditions (ICP forward power, central channel gas flow rate and sampling position), Lee et al. [59] calculated that SiO_2 and PbO particles up to 250 nm would be completely vaporized, whereas Au and Yb_2O_3 particles should have sizes below 150 and 100 nm, because of their higher density and boiling point, respectively. Considering that the degree of ionization depends on the plasma conditions and the ionization potential of the element, incomplete vaporization of large particles has been reported by a number of authors even under optimized conditions. This has been the case for Au particles of 250 nm [59] or for SiO_2 particles over 1.8 μm [55]. In the case of polystyrene microparticles, it has been confirmed that particles up to 5 μm were totally vaporized [40].

The size of the ion cloud, and hence the time-width of the signal produced from a particle, arises mainly from the extent of diffusion of the ion cloud. Once a particle is completely vaporized, the width of the signal will increase with the residence time, due to more time for diffusion, if the center gas flow rate or the sampling position are decreased [55]. Thus, smaller particles are subjected to diffusion to a greater extent because they are completely vaporized early in the plasma. Because only ions that are sampled near the center of the sampling orifice will be extracted and detected, diffusion of ions off-axis will reduce the fraction of ions detected per particle [55]. Ho et al. [57] studied the effect of boiling points and diffusion coefficients on the particle signals, predicting that particles with higher boiling points and high-mass/slow-diffusion elements will show higher sensitivity.

In their travel through the plasma, droplets follow different trajectories (and hence different residence times) depending on the entrance radial position, which affects the volatilization of particles and the diffusion of ions [60]. A computational study confirmed the advantages of on-axis introduction of particles to achieve higher transport efficiencies and signals [56]. On the other hand, samples are typically introduced as polydisperse aerosols, which means that the complete desolvation of droplets with different initial diameters occurs at different times/locations in the plasma. Smaller droplets are desolvated before than larger ones; therefore, particles will be completely vaporized before, and the resulting ion clouds will have more time for diffusion before being extracted through the interface. In the end, all these factors can produce variations in the intensity and duration of the signals from particles of the same size and therefore resulting in the broadening of the original size distribution of the particles [10]. This broadening effect has been reported for Au nanoparticles [5,61] and it has been specially significant for polystyrene microparticles [40].

In view of the processes discussed above, the location in the plasma of maximum ion density involves that particles are fully vaporized and highly ionized, and needs to be similar for both the particle in the sample and the standard used for size/mass per particle calibration. This suggests that size calibration should be done with particles of the same composition and known size, rather than dissolved standards, which probably would exhibit different behavior in the plasma [58,59]. However, standard monodisperse particles may not always be available, and dissolved standards of the monitored element are routinely used. In this case, the analyte transport efficiency and the sample flow rate must be known, assuming that the transport and the overall ionization efficiency is the same for dissolved and particulate forms, producing the same signal intensity per unit mass of element. In this regards, Ho et al. [62] reported a shift in the maximum sensitivity location for 80 nm ZrO_2 nanoparticles in comparison with a Zr dissolved standard. This was also the case for 250 nm Au nanoparticles, whereas for 150 nm nanoparticle the location was similar to the dissolved standard, suggesting that sampling position profiles must be optimized to obtain accurate results when using dissolved standards. Kinnunen et al. [63] performed an experimental design to study the effect of the nebulizer gas flow rate, plasma power and sampling position on Au sensitivity by using Au(III) and 50 nm Au nanoparticles. Although some differences in the behavior of the particles and the dissolved element were observed as regard to sampling position, similar optimal conditions could be selected to use Au (III) as standard in SP-ICP-MS analysis.

Accurate sizing of Au nanoparticles has been demonstrated by using dissolved standards for a wide range of diameters from 20 to 200 nm [61,64]. In a similar way, an interlaboratory study involving the sizing of Au nanoparticle reference materials (RM 8012 and RM 8013) also showed the reliability of this calibration mode in SP-ICP-MS [65]. Alternatively, if a monodisperse droplet generator is used [23,66], solutions containing known concentrations of the dissolved element could be used for calibration if the particle formed after droplet desolvation behaves in a similar way than the nano or microparticles, as discussed above.

4. Collision/reaction cells

While ICP-MS has proven to be a powerful technique in the analysis of nanomaterials, it suffers from some limitations, which are hence applicable to SP-ICP-MS. As in ICP-MS, the presence of spectral interferences coming from the sample matrix but also from the plasma itself should be carefully considered and studied to give reliable results. Spectral interferences are produced by atomic and/or polyatomic ions with the same mass-to-charge (m/z) ratio as the target element. Isobaric and matrix/plasma polyatomic interferences contribute to a higher background signal, which usually hampers the feasibility of SP-ICP-MS to identify smaller particles, and therefore increasing the size detection limits [37]. The use of double focusing mass analyzers which will be discussed in the following section, is a good approach to avoid spectral interferences due to their higher spectral resolution [67]. Alternatively, this problem has usually been overcome in quadrupole ICP-MS by selecting less-interfered isotopes or using mathematical corrections, although the use of collision/reaction cells alone [68] or in combination with a previous quadrupole (ICP-MS/MS) has become widely used [69,70,71] . Collision/reaction cells consist of a multipole placed before the quadrupole mass analyzer, pressurized with a gas in which polyatomic interferences collide with an inert gas (He) followed by kinetic energy discrimination (KED) or with a reaction gas (H_2, O_2, CH_4, NH_3, CH_3F) which reacts with either the target element (mass-shift approach in ICP-MS/MS) or the interference (on-mass approach in ICP-MS/MS). Although the use of collision/reaction cells is well established in conventional ICP-MS, the number of works dealing with spectral interferences in SP-ICP-MS is still scarce. The majority of SP-ICP-MS studies are based on elements mostly free of spectral interferences, as it is the case of Au and Ag nanoparticles. However, the increasing interest in different sorts of nanomaterials containing elements that suffer from spectral interferences in ICP-MS, has opened new challenges for SP-ICP-MS analysis. The use of He as collision gas has been reported in the determination of Al_2O_3 [72], Fe_3O_4 [73], TiO_2 [74] and ZnO nanoparticles [75,76] in different kind of samples. On the other hand, O_2 has been studied in the detection of SiO_2 [77] or TiO_2 nanoparticles [78], whereas mixtures of O_2 and H_2 have been used in the successful determination of TiO_2 nanoparticles [17,75,79]. H_2 has been proposed in the study of Fe [80], Se [81] or SiO_2 nanoparticles [75,77,82] and NH_3 has been used in the analysis of Cr [75], Cu [75,83], ZnO [83], SiO_2 [75,77,84], Fe [75,85,86] or TiO_2 nanoparticles [83,87]. The

applicability of cell gases for "on-mass" (H_2 for ^{12}C and ^{13}C) and "mass shifting" (H_2 (m/z to $m/z + 1$), O_2 (m/z to $m/z + 16$) and NH_3 (m/z to m/z + 15, 16, 17, 18) analysis via SP-ICP-MS/MS in polystyrene-based microplastics detection in ultra-pure water and seawater has been also explored [88]. In general, ion transmission was lower for mass shifting MS/MS methods compared to both C isotopes on-mass with or without gas, with H_2 as the cell gas with the highest ion transmission and best size detection limit monitoring ^{12}C. If higher selectivity is required, O_2 as cell gas achieved the highest ion transmission and best size limit of detection monitoring a to $m/z + 16$ mass shift. As much appealing as the use of collision/reaction cells might be found, thorough evaluation and considerations of the effect of the gases on the nanoparticle signals should be taken into account. Ion clouds from nanoparticles behave in the cell quite differently from dissolved analytes, being the ion cloud enhancement from metallic nanoparticles much larger than that observed for dissolved analytes. Comparison with conventional ICP-MS led to the need for lower reaction gas (NH_3) flow rates for the analysis of nanoparticles than for dissolved metallic ions [68,83]. Not only a careful optimization of the gas flow rate and the different parameters in the cell should be considered, but also the dwell time and/or nanoparticles size and nature, given that they might have an impact on the duration of the nanoparticles signals too [83,86]. Different works show how the use of gases led to a significant broadening of the nanoparticles signal [83,86,89,90], being this effect more significant in the case of heavier and more reactive gases (e.g., NH_3 or O_2) than for lighter ones (e.g., H_2 or He). Bolea-Fernandez et al. [86] reported Au nanoparticles transient signals widths of 600 μs in "no gas" and H_2 modes, with a slight increase to 700 μs in He mode and a drastic change to 2590 μs and 1840 μs in the case of NH_3 (on-mass and mass-shift approaches, respectively), and for which a significant peak tailing was also observed. In this same work, 200 nm Fe_3O_4 nanoparticles experienced a signal duration of 940 μs when using H_2 while this duration was 6000 μs for NH_3. More recently, Suárez-Oubiña et al. [83] reported broader signals when measuring TiO_2, Cu, CuO and ZnO nanoparticles with NH_3 as reaction gas, observing that peak widths were strongly dependent on the ion product selected (broader peaks obtained for the largest ion products). The significant differences observed between the use of NH_3 and the other gases was attributed to the larger size of NH_3 molecules compared to H_2 molecules and/or He atoms. The larger size would increase the probability of collision/interaction with the ion cloud of each nanoparticle event, making some of the ions lose kinetic energy and hence, being detected at different moments. In order to accelerate the product ions generated in the collision/reaction cells an axial acceleration feature has been incorporated in some instruments to increase the kinetic energy of these reaction product ions, enhancing their transport out of the cell into the quadrupole mass analyzer. Axial acceleration has been used in the determination of Cr, Cu, Fe, Si, Ti and Zn nanoparticles [75] and was found to be crucial to resolve TiO_2 signals from the background [17]; however, an improvement in signal width was not observed when applied to the analysis of Fe_3O_4 nanoparticles [86]. Special attention should be paid to this broadening effect, since it could make it difficult to discriminate particle events from the baseline, compromising their detection [75] and/or leading to a biased determination of the particle number concentration and size.

Although the increase in the signal peak width of nanoparticle events using collision/reaction cells might be seen as an important drawback if not carefully considered, it also opens new possibilities to monitor multiple elements in single particles using quadrupole ICP-MS instrumentation, as it will be discussed in the following section. This approach has been used successfully for the simultaneous quantification of two elements by SP-ICP-MS using a quadrupole-based system [89,91]. In these cases, the use of gases with larger collisional cross-sections (e.g. NH_3) is favored since they induce a larger peak broadening, as discussed by Bolea-Fernandez et al. [86].

5. Mass analyzers

The mass analyzers used in commercial ICP-MS instruments are quadrupole, double focusing (DF) or time-of-flight (TOF). Among all of them, quadrupole-based instruments (ICP-Q-MS) are the most commonly reported in literature for single particle detection as they are widely used due to their lower cost and higher robustness. However, since quadrupoles are sequential analyzers, only one m/z can be monitored at a time. Switching between different m/z requires a settling time for stabilization of the motion of ions once quadrupole voltages change when moving from one m/z to another, meaning integration windows are not continuous and implying a fraction of signal/ions being lost [92]. Despite these limitations, it is possible to monitor two m/z during the duration of each individual particle event, implementing a higher data acquisition frequency capability, working at dwell times in the microsecond range, and improving the capability for transmission and storage of data [93]. Under such conditions, dual-element detection of Au core/Ag shell nanoparticles was successfully reported by Montaño et al. [92] using 100 μs dwell time and 100 μs settling time (shorter settling times caused a drop in signal intensities since mass analyzer electronics switched faster than ions to clear the analyzer). More recently, peak broadening obtained by the use of O_2 collision gas was used for dual m/z measurement of Ag nanoparticles, and further applied to determine isotope ratios of individual particles [89]. For this purpose, a model for the selection of optimal peak width based on the sampling period of the spectrometer (settling time and dwell time) was proposed. These authors recommended elements with atomic mass >90 for dual m/z measurement and a difference in m/z between two isotopes smaller than 20. In this work, limitations regarding high size limit of detection and number of isotopes monitored were a consequence of the longer settling time (500 μs) the quadrupole required. In any case, these dual-monitoring capabilities are still not commercially available in ICP-Q-MS instrument. On another front, since only a small fraction of the generated ions reaches the detector, efforts have been put in improving ion transmission through the mass spectrometer to decrease size detection limits. Optimization of ion lenses parameters and manipulation of the mass bandwidth of the quadrupole have been studied for this purpose. Increasing the mass bandwidth of the quadrupole mass filter resulted in a decreased mass resolution and an increased ion transmission, providing equivalent size detection limits of 4.2 nm for Au nanoparticles, and 5.7 nm, 20.1 nm, and 12.2 nm for Gd, Er, and Yb present in lanthanide-doped up-conversion nanoparticles [94].

As in the case of quadrupoles, double focusing are also sequential analyzers. Although this kind of instrumentation has not been so widely used in the analysis of nanomaterials, its highest sensitivity and mass resolution, as well as the recent feasibility of using dwell times down to 10 μs with instruments of last generation [95], have made ICP-DF-MS a competitive option for the detection of nanoparticles [96–100]. When comparing the performance of double focusing and quadrupole instruments, it was observed that the increased sensitivity of the former resulted in a decrease in the size detection limit from 17.8 nm to 4.9 nm for Ag nanoparticles, which were further improved using dry aerosols, which led to a higher efficiency of the ion extraction from the plasma, resulting in size detection limits of 3.5 nm for Ag and 12.1 nm TiO_2 nanoparticles [101]. Similarly, a 200-fold improved sensitivity and 4-fold decreased size detection limits were reported for Ce, when compared to the use of ICP-Q-MS, leading to size detection limits below 4.0 nm for CeO_2 nanoparticles [102]. Furthermore, ICP-DF-MS has proven to be an extraordinary approach for removing spectral interferences. To deal with the spectral overlap of Ar-based polyatomic interferences with Fe, pseudo-medium resolution mode was selected in a last generation double focusing instrument working at dwell times of 50 μs for the successful characterization of iron oxide nanoparticles, Fe_3O_4. Size detection limits of 19 nm were obtained, which were comparable to the ones obtained by using H_2 (on-mass) in ICP-MS/MS [85]. Additionally, TiO_2 nanoparticles were detected in calcium rich matrices, as

typical for natural waters, by using the most abundant isotope ^{48}Ti and high-resolution mode in an ICP-DF-MS instrument [87]. Size detection limit of 10 nm in ultrapure water was achieved with this instrumentation working at millisecond dwell times, in comparison to the 64 nm obtained when using NH_3 and ICP-MS/MS. Moreover, this high resolution ICP-DF-MS allowed measuring TiO_2 nanoparticles at Ca concentration up to 100 mg L^{-1}.

To overcome the multi-element limitations of quadrupole and double focusing instruments, the use of time-of-flight mass analyzers has found its way in the analysis of nanomaterials [103,104] in part due to specific improvements developed within the last decade. All currently commercially available ICP-TOF-MS instruments have shown their feasibility in SP-ICP-MS analysis [102,105–108] . Although these instruments have similar TOF designs, they differ in terms of mass range, sensitivity, and mass resolution. For further comparison and figures of merit of the different commercially available ICP-TOF-MS instruments that have been used for SP analysis, the reader is referred elsewhere [104]. When compared to other mass analyzers, equivalent (or even smaller) size detection limits have been observed between ICP-Q-MS and ICP-TOF-MS [105]; whereas higher sensitivity of double-focusing instruments resulted in a lowering of the size detection limits from 34 nm to 15 nm for TiO_2 nanoparticles in ICP-TOF-MS and ICP-DF-MS, respectively [108]. In this line, size detection limits of 16.8 nm, 11 nm and below 4 nm were reported for CeO_2 nanoparticles using ICP-Q-MS, ICP-TOF-MS and ICP-DF-MS, respectively [102]. Undoubtedly, the main advantage of this kind of instrumentation lies in the simultaneous multi-element capability, being able to register nearly the whole mass spectrum within each reading [109]. However, considerations should be taken if an element is not detected in a multielement particle, such particles could be falsely identified as single-element ones [107]. SP-ICP-TOF-MS has shown to be a useful technique for classification of nanoparticles containing the same major element based on their multi-element fingerprint. In this sense, engineered CeO_2 nanoparticles have been successfully distinguished from natural [110] and incidental [107] Ce-containing nanoparticles. In the engineered CeO_2 nanoparticles only Ce was detected, whereas in the naturally occurring ones other elements, typically other rare earth elements (La, Pr, Nd, Th), were present. Distinction between natural and incidental nanoparticles was based on the different Ce:Nd mass ratios. Multi-elemental analysis revealed that natural TiO_2 particles in surface waters are often associated with at least one other element (Al, Fe, Ce, Si, La, Zr, Nb, Pb, Ba, Th, Ta, W or U) [106], although no specific multi-element signatures were confirmed for engineered TiO_2 nanoparticles [103]. Industrial relevant nanoparticles such as Ti and Nb carbonitride particles from microalloyed steels [111], bismuth vanadate ($BiVO_4$, used as pigment), sodium titanate ($(Bi_{0.5}Na_{0.5})TiO_3$, used as ceramic materials) and steel platelets (containing Fe, Cr, Ni, Mo) [105] have also been studied by SP-ICP-TOF-MS. Because of its multi-elemental character, the large amount of data generated by SP-ICP-TOF-MS requires automated and robust data processing strategies to reduce the inherent complex datasets to interpretable data. For this purpose, machine learning and clustering analysis have been proposed [112] to better understand and classify the origins of various particle types present in environmental samples.

6. Detection

Secondary electron multipliers (SEM) are the most common detectors used for ICP-MS with quadrupole and double focusing mass analyzers. In standard ICP-MS, these fast and sensitive detectors are designed to work in dual mode, switching from pulse counting to analog mode when ion currents larger than a certain threshold are detected [113]. In analogue mode, the SEM is operated in a medium amplification range and the resulting current is measured using conventional low-current amplification techniques. Working at higher amplification range, individual electron pulses can be readily detected and counted using sensitive pulse counting electronics. In SP-ICP-MS, data are normally collected in pulse counting mode as the time required for the pulse to analog conversion would result in unrecorded signal, especially when working at microsecond dwell times [84]. The counting stage of this kind of detectors is limited due to the non-linear response caused by the overlapped arrival of ions at the detector within the dead time of the multiplier detector and pulse counting electronics (i.e. pulse pile-up) [59], which results in relevant count losses. The deviation of the detector response can be estimated using Poisson statistics and the true count rates calculated according to the dead time and the characteristics of the counting circuitry [114]. A correction procedure is commonly implemented by the data processing software of commercial ICP-MS instruments, although in the case of SP-ICP-MS some particularities should be considered in addition. Whereas in standard ICP-MS the signals managed hold constant count rates along the reading time, when ICP-MS is operated in single particle mode, the count rate varies along the particle event and it can exceed the pulse counting range within the dwell time in spite of the average count rate being lower [55,59]. Under such conditions the conventional dead time correction will underestimate the true counts of the reading, underestimating the content of the element and hence the particle size. This non-linear response in SP-ICP-MS analysis has been predicted to occur for Au nanoparticles larger than 70 nm [64]. Lee et al. [59] observed a deviation from linearity of 250 nm Au nanoparticles, being limited up to 150 nm. However, larger size linear ranges have been reported for Au nanoparticles, up to 250 nm working at lower sensitivities [115]. Strenge and Engelhard [114] pointed out the relevance of the dead time correction by using a custom data acquisition system working at milli- and microsecond dwell times. Moreover, they reported larger linear dynamic ranges when applying dead time correction using microsecond than millisecond dwell times.

Alternatively, and in view of the limited dynamic range of pulse counting SEM detectors reported so far, different approaches to reduce the overall sensitivity without modifying the detector parameters have

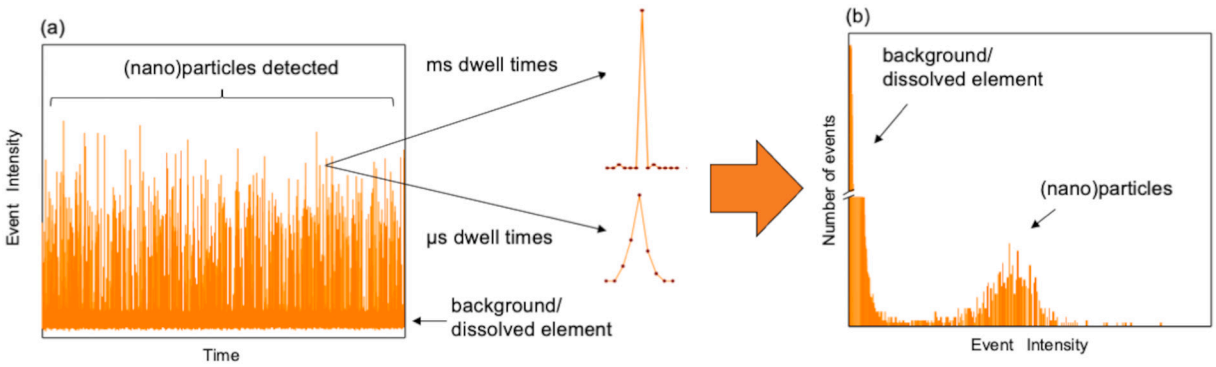

Fig. 4. SP-ICP-MS time scan (a) and intensity histogram (b) of a suspension containing nanoparticles and dissolved forms of the same element. The time scale of the (nano)particle event recorded at microseconds dwell times x100.

been proposed. They include the use of less abundant isotopes [40], the attenuation of the signals by defocusing the ion beam [114] or the use of collision gases under kinetic energy discrimination [64,90] to extend the upper dynamic range of particle size.

On the other hand, detectors based on microchannel-plate detectors, commonly used in time-of-flight instruments, can be optimized for the dynamic range required, allowing short periods of significantly higher count rates, as it may happen with nanoparticle signals [95]. Signals equivalent to 3×10^7 cps have been reported without detrimental effects with this kind of detectors with data acquisition frequencies up to 10^5 Hz and low dead times (10 ns), using an attenuation grid prior to the entrance to the detector, which can produce attenuation factors between 120 and 400 depending on the grid.

Faraday detectors, present in multicollector instruments, have also been used in single particle mode to measure isotope ratios of individual erbium oxide particles in the range from 130 nm to 3 μm [116], as well as silver nanoparticles with sizes between 40 and 200 nm [117]. With these type of detectors, wide dynamic ranges are possible because of their capability to monitor high-count rates signals larger than 10^8 cps. Besides, they are free from counting losses due to dead time in contrast to electron multipliers. However, the response of the Faraday detectors is much longer, because of the time constant used in the dc amplification process to measure the ion current (integration times of 0.1 s have been reported), which implies longer total acquisition times (as long as 30 min) and requires working at lower number particle concentrations (e.g., 70 particles per mL) to avoid the overlapping of two or more particle events.

7. Data acquisition

SP-ICP-MS measurements are performed in time resolved mode, producing bidimensional signals (Fig. 4a), where the intensity of individual readings is recorded versus time. The output is a time scan in which a number of particle events are shown above a continuous baseline, which is due to the background at the m/z recorded or the presence of dissolved forms of the element measured. The data acquisition frequency is at the core of single particle detection, always in combination with the analysis of suspensions at low number concentrations. If the duration of a typical particle event is in the range of 300–1000 μs [58], suitable dwell times must be short enough to detect particle events individually. At the beginning, commercial quadrupole instruments could only work with dwell times in the millisecond range, being recommended 3–10 ms. Under such conditions, individual particle events are detected within a dwell time period and recorded as pulses (or 1-reading events), minimizing the recording of events involving two or more particles when using longer dwell times, or the partial detection of particles when shorter ones are used. The following generation of commercial instruments was specifically designed to support the single particle detection capability, increasing the data acquisition rate by shortening the applicable dwell times down to 10 μs with quadrupole [93] and double focusing [95] instruments. By using microsecond dwell times, particle events are recorded as peaks consisting of a number of readings (maximum dwell times of 100–200 μs are recommended to obtain at least ca. 3 readings along the peak). Although the development of data acquisition systems with dwell times down to 5 μs have been reported [118], modelling of size detection limits with respect to dwell time has shown that best size detection limits are achieved when using microsecond dwell times in the upper range of 100–200 μs [6,119], as discussed below.

The advantages of using microsecond dwell times have been highlighted in a number of papers [6,37,92,93,95,119]. By using microsecond dwell times, higher fluxes of particles, and hence higher particle number concentrations, can be used while maintaining the low occurrence of 2-particle events [37]. The option of working at higher number concentrations t allows to improve the precision due to counting statistics, to reduce the bias due to 2-particle events and hence to increase the number concentration dynamic range [37,92,119]. On the other hand, dwell times have a drastic effect on the baseline count-intensity and its associated noise that affect size (and mass per particle) detection limits. This is especially important for high baselines due to polyatomics or the presence of dissolved species of the element measured [37,95].

The effect of dwell times on size (and mass per particle) detection limits is not straightforward. When using millisecond dwell times, the intensity of the particle events, which are recorded as pulses, is independent of the dwell time; thus, size (and mass per particle) detection limits only depend on the baseline noise (equal to the square root baseline intensity), which are reduced proportionally to the square root of the dwell time. However, for microsecond dwell times, the maximum intensity of recorded peaks decreases with the dwell time, which means that size (and mass per particle) detection limits increase with the square root of the dwell time used [6]. Despite this inverted behavior of the size (and mass per particle) detection limits when using milli and microsecond dwell times, lower detection limits are achieved when using microsecond dwell times [6,92,119]. On the other hand, the use of short microsecond dwell times offers a novel feature to quadrupole SP-ICP-MS, providing sequential detection of two elements in the same particle, although the quadrupole mass analyzer settling time has to be still considered in this case [92], as it has been discussed in a previous section.

Moving one step forward, Duffin et al. [120] have proposed a new strategy for single particle detection by acquiring data with dwell times below 10 μs. Instead of detecting the particle events through the signal intensity rising over the baseline, discrimination of particle events is accomplished by analyzing the difference in the arrival time between successive ions. The closely spaced arrival of ions from the particles differs from the Poisson ion arrival distribution of background ions or ions resulting from continuous sample introduction, enabling the identification of the particles. This novel approach has proven its capability for detection of small nanoparticles over a high background, although it still requires further investigation.

8. Signal processing

Raw time scans (Fig. 4a) can be processed by plotting the particle event intensity (the sum of the individual readings along the particle event) against their frequency, obtaining histograms as shown in Fig. 4b, where the first distribution is due to the background and/or the presence of dissolved forms of the element measured and the second one to the particles themselves.

The differentiation between baseline and particles may not be so evident as in Fig. 4b, and more robust criteria for discrimination of baseline and particle events must be applied, as those based on thresholds related to the baseline noise. Although a 3-sigma criterion was initially proposed by Pace et al. [16], and coefficients up to 8 have been applied, Laborda et al. [6] have demonstrated that a 5-sigma criterion avoid the occurrence of false positives in most acquisition conditions. These widely-used criteria are based on the Poisson or Poisson-normal behavior of baseline signals measured in quadrupole and double focusing instruments, which are equipped with electron multiplier detectors; however, they must be adapted in the case of time-of-flight instruments, because of the compound Poisson behavior shown with microchannel plate detectors [121]. On the other hand, when particle events are recorded as peaks, approaches similar to those applied to the detection of chromatographic peaks have been used [95,122]. Whereas particle events detected as pulses are easily handled by using simple algorithms implemented in spreadsheets [123], processing of peaks involves more complex algorithms and software [95]. ICP-MS manufacturers have developed their own proprietary software for data processing and a number of authors have also reported the development of different custom scripts, although not always freely available. To the best of our knowledge, only the free-software SPCal is currently

available [124]. In any case, the accuracy of current SP-ICP-MS analysis, as in chromatography, relies on the software used, which should also be conveniently validated [125].

Additional methods for data treatment to cope with specific problems have also been developed. Cornelis and Hassellöv [126] proposed a signal deconvolution method to improve the detection capability of small nanoparticles when overlapping between baseline and particle signals occurs. Cornelis and Rauch reported an algorithm based on a moving average to correct the drift of the baseline [127]. Specific algorithms for peak recognition of particle events recorded at microsecond dwell times have also been proposed [119,128].

Whereas in nebulization SP-ICP-MS the baseline signal is constant, this is not the case in LA-SP-ICP-MS because of the heterogeneous distribution of the dissolved forms of the target element in the ablated matrices [51,124]. Lockwood et al. [124] proposed the use of a dynamic (rolling median) threshold criterion, instead of the conventional static one, for detection of microplastics dispersed in a soil matrix. For imaging and mapping of biological tissues, Metarapy et al. [51] developed an algorithm for processing the individual data of each pixel measured in combination with a visualization application to show the spatial distribution of dissolved and nanoparticulate silver, as well as the size and number concentration of the nanoparticles, in sunflower root sections.

9. A summary of benefits and limitations

ICP-MS is a well-established ensemble technique that provides elemental and isotope ratio information in a wide variety of samples within a broad range of concentrations, down to the parts per trillion. By incorporating the capability of performing continuous measurements at frequencies over 100 Hz to commercial instruments, ICP-MS also became a particle counting technique, expanding its performance, and making SP-ICP-MS accessible to any laboratory with ICP-MS instrumentation. The interest shown by ICP-MS manufacturers in single particle detection has been key to its success and further development. Hence, the technique has moved into new analytical dimensions not foreseen years ago. Nowadays, the use of an ICP-MS instrument in single particle mode allows the detection, characterization and quantification of nano and microparticles, mostly inorganic but also organic, in different types of samples. In a relatively quick way, information about the different forms of the element (dissolved, nano, and/or micro), as well as mass/size distributions can be obtained. Moreover, it is also useful when it comes to detect or monitor changes of the nanomaterials (e.g., agglomeration, aggregation, dissolution) or even to establish the natural or anthropogenic origin of some nanomaterials with instruments of simultaneous multi-element capability. A recent revision [13] has shown that the number of analytical applications of the technique is steadily growing, being frequently applied in laboratory studies about fate and (eco)toxicity of nanoparticles, as well as to the analysis of samples originally containing nanoparticles, namely foods, environmental and biological samples. In any case, the increasing relevance of the technique lies in its outstanding performance, that covers particle size ranges from few nanometers to several micrometers at concentrations down to hundreds of particles per milliliter.

Like any other analytical technique, SP-ICP-MS not only offers benefits, but also suffers from limitations. Although some of them are intrinsic to the technique itself, there is still room for improving others in the future. Definitely, the element-specific nature of ICP-MS constitutes the main intrinsic limitation of SP-ICP-MS, because, in principle, the technique provides only information about the mass of the element(s) in each particle, but not about its morphology (size and shape) or composition. This means that SP-ICP-MS must rely on the information from other techniques to transform the element mass into size once the shape, composition and density of the particles are known; otherwise, these characteristics must be assumed and hence only equivalent sizes can be reported (e.g., equivalent diameters if spherical shape is assumed). However, this limitation has not prevented the differentiation of pristine nanoparticles with different shapes (spheres and rods) by analyzing the time profiles of the particle events [129].

Although SP-ICP-MS mostly involves the analysis of liquid suspensions, its combination with laser ablation has opened the way to the direct analysis of solid samples. However, the main limitation of LA-SP-ICP-MS lies in the risk of particle degradation during the ablation process, which must be prevented by using low laser fluences, below the ablation threshold of the matrix involved. With this constraint, the analysis of solid samples is restricted to biological matrices, whose ablation thresholds are generally lower than 1 J cm^{-2}. With regard to inorganic matrices, its application is restricted to the analysis of powered samples (e.g., sediments, soils), where the laser irradiation is used as a way of introducing into the plasma target particles dispersed into the sample or the sample particles themselves with minimal degradation.

Minimum size attainable is given by the detection efficiency of the instrument (the ratio between the number of ions detected and the number of atoms introduced into the plasma), which depends, in turn, on the transmission of the ions through the spectrometer. In this regard, double focusing spectrometers offer the best size detection limits under low resolution conditions because of their higher transmission, so future improvements in this feature will result in the further reduction of these detection limits. Improvements on the minimum detectable number concentration implies an increment on the number of particles entering the plasma through the sample introduction system per time unit, which depends on the nebulization efficiency and the sample flow rate. Although 100% nebulization efficiencies can be achieved, these systems require very low sample flow rates and the ultimate reduction of these detection limits lies in extending the measuring times.

While most efforts are usually focused on lowering detection limits, the upper dynamic ranges cannot be ignored. Incomplete volatilization can cause the underestimation of the size of large particles if the plasma conditions (ICP power, central channel gas flow rate and sampling position) are not adequate to the nature of the nanoparticles, in particular to their density and boiling point of their components. Even in the case of the complete volatilization of the nanoparticles, the rapid increase of the count rates within the duration of the particle events can exceed the pulse counting range of conventional detectors, leading to the underestimation of their size as well. In spite of these limitations, large particles made of low density/boiling point substances (e.g., plastics, silica/silicates) can be analyzed by selecting the adequate isotope to control the sensitivity required. In such cases, the maximum feasible sizes are still in the range of several micrometers, because of the lower efficiency of current nebulization systems for larger particles. Similarly to what happens with size, the analysis of suspensions with high number concentrations is prone to biased results because of the particles coincidence, which involves that two or more particles may be recorded as a single one of larger size, distorting the original size distribution and underestimating the number concentration. When liquid suspensions are analyzed by SP-ICP-MS, dilution can be used to modify the concentration of nanoparticles and hence control the recording of 2-particle events. However, in LA-SP-ICP-MS this limitation must be circumvented through instrumental control [50]. In this respect, regarding the laser-beam size, as the number of particles detected is proportional to the area ablated per laser pulse, the reduction of the beam size can serve for "dilution" and it is a straightforward way to avoid detection of 2-particle events. The same effect can be obtained by reducing the repetition rate.

A limitation that is not exclusive to SP-ICP-MS but concerns the analysis of nanoparticles in general is the lack of standards of most of the particles analyzed, especially in relation with size and composition. This limitation is circumvented in SP-ICP-MS by the determination of the nebulization efficiency and the calibration with dissolved standards of the element monitored, assuming the same behavior than in particulate forms. The reliability of the methods available for the determination of the nebulization efficiency has been evaluated recently [18] and elements typically analyzed by SP-ICP-MS (Ag, Au, Ti, Cu…) show similar

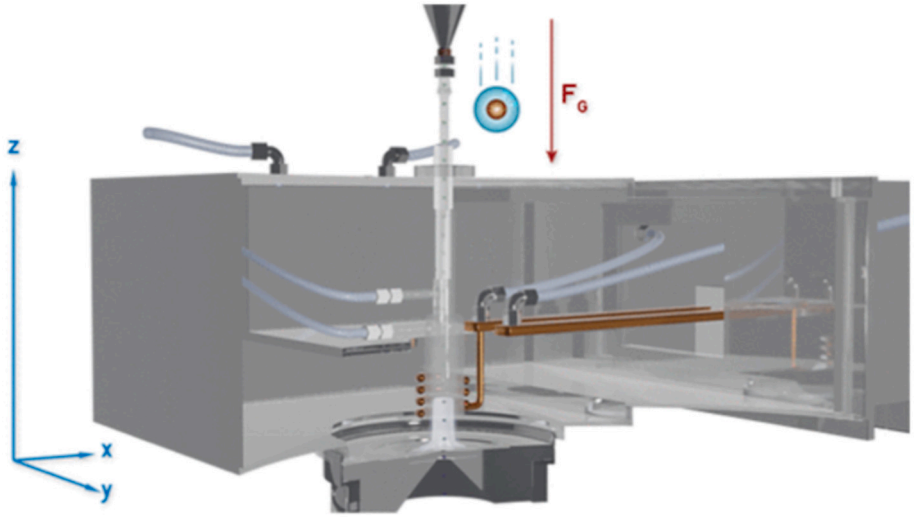

Fig. 5. Schematic drawing of a downward-pointing ICP-MS prototype in combination with a microdroplet generator [136]. With permission from the American Chemical Society.

sensitivities regardless of their physicochemical forms, although it should be checked for larger particles, as well as for more refractory elements.

A last limitation that cannot be disregarded is the need of harmonized criteria and tools for signal processing. This lack of agreement is evidenced in the diverse criteria adopted by the different authors across publications for handling baselines and identification of particle events, which also affects to the evaluation of detection limits. In turn, this has a direct implication on the computer programs developed for signal processing, which are now supplied primarily by the manufacturers as part of their specific software for single particle analysis. These programs are utilized by users in a similar way than those for chromatography, although with less flexibility and without the possibility of comparing results between programs. In this regard, it would be highly recommended the availability of validated open-source software that could incorporate different data processing strategies and that would be accessible to any user regardless of the instrument employed.

10. Future perspectives

Although SP-ICP-MS has focused on the analysis of inorganic nanoparticles, with external dimensions below 100 nm, there is a recent trend toward the analysis of bigger particles such as plastic particles [40,88,124,130] by monitoring carbon isotopes or carbon polyatomics. Due to the higher limits of detection attainable for carbon in ICP-MS, the current range of detectable particles is over ca. 1 μm [40], which requires the utilization of high throughput sample introduction systems. This has led to the substitution of conventional nebulization systems, based on cyclonic or double-pass spray chambers, by linear-pass spray chambers equipped with microflow nebulizers, which were originally designed for single-cell ICP-MS analysis.

The incorporation of microplastics to the catalogue of particles that can be analyzed by SP-ICP-MS opens new challenges and perspectives in the field, because of the inherent difficulties for nebulizing and vaporizing such large particles but also for the unbiased detection of the clouds of ions that are generated. In this regard, it has been shown that polystyrene microparticles up to ca. 2 μm were nebulized with the same efficiency than Au nanoparticles by using of a microflow nebulizer in combination with a linear-pass spray chamber, whereas the transport efficiency dropped by half for 5 μm microparticles [40]. On the other hand, the use of the less abundant isotope ^{13}C allowed to keep signals under the working range of the pulse count detector up to ca. 5 μm [40].

Whereas microplastics have their three dimensions in the microscale, other particles with one or two dimensions in the nanoscale and the others in the microscale (nanotubes/nanorods/nanowires or nanoplates, respectively) can be handled also in SP-ICP-MS following a similar approach to that of microplastics. In fact, silver nanowires [131], nanoclays (monitoring Al) [132] and carbon nanotubes (monitoring Y impurities) [133–135] have been analyzed by SP-ICP-MS using conventional nebulization systems, although only providing qualitative or semiquantitative information. More recently, the validated quantitative analysis of nanoclays with lateral dimensions below 1 μm, has been reported by combining the use of a high transport efficiency nebulization system and modulating the ^{27}Al sensitivity to cover the whole size range of the nanoclays analyzed [41].

The analysis of particles with micrometer dimensions may not produce quantitative results with all types of particles in spite of the application of different approaches cited above. However, SP-ICP-MS can always be used for the rapid screening of samples to detect the presence of particles over a certain size at low number concentrations, which should be submitted to further analysis by more demanding but also more selective techniques.

Regarding microparticle nebulization, the commercialization of high transport efficiency nebulization systems by a number of manufacturers will contribute to further development in the area, as should also happen with the microdroplet generator, which has recently been commercially available. In this respect, the sustained research on sample introduction by microdroplet generation has led also to the development of downward-pointing vertical ICP-MS instruments for their combined use with this sample introduction systems [136,137], as it is shown in Fig. 5. This novel approach allows the gravity-assisted introduction of the sample from the top, expanding the sample transport capabilities of large droplets and particles regardless of their size. Although primarily intended for single cell analysis, its application to the analysis of single nano- and microparticles may be also promising.

The analysis of organic particles as well as of large particles can be considered next challenges and future steps in SP-ICP-MS. However, these difficult tasks are closely linked to the introduction of such particles into the spectrometers, which in the end is the everlasting Achilles heel of atomic spectrometry. SP-ICP-MS is not free from this “curse” and the development of new sample introduction approaches or the adaption of existing old ones, both for liquid and solid samples, is without a doubt an underlying and crucial issue also for SP-ICP-MS.

Declaration of Competing Interest

The authors declare that they have no known competing financial interests or personal relationships that could have appeared to influence the work reported in this paper.

Data availability

No data was used for the research described in the article.

Acknowledgements

This work was funded by the Spanish Ministry of Science and Innovation (MCIN/AEI/10.13039/501100011033), project PID2021-123203OB-I00, "ERDF A way of making Europe" and the Government of Aragon, project E29_17R. IAA thanks the European Union-Next Generation EU and the Spanish Ministry of Universities for funding under the María Zambrano Grant (MZ-240621).

References

[1] F. Laborda, E. Bolea, G. Cepriá, M.T. Gómez, M.S. Jiménez, J. Pérez-Arantegui, J. R. Castillo, Detection, characterization and quantification of inorganic engineered nanomaterials: a review of techniques and methodological approaches for the analysis of complex samples, Anal. Chim. Acta 904 (2016) 10–32, https://doi.org/10.1016/j.aca.2015.11.008.

[2] C. Degueldre, P.-Y. Favarger, Colloid analysis by single particle inductively coupled plasma-mass spectroscopy: a feasibility study, Colloids Surfaces A Physicochem. Eng. Asp. 217 (2003) 137–142, https://doi.org/10.1016/S0927-7757(02)00568-X.

[3] L. Ebdon, M. Foulkes, K. Sutton, Slurry nebulization in plasmas, J. Anal. At. Spectrom. 12 (1997) 213–229, https://doi.org/10.1039/a604914a.

[4] L.A. Currie, Limits for qualitative detection and quantitative determination: application to radiochemistry, Anal. Chem. 40 (1968) 586–593, https://doi.org/10.1021/ac60259a007.

[5] F. Laborda, J. Jiménez-Lamana, E. Bolea, J.R. Castillo, Critical considerations for the determination of nanoparticle number concentrations, size and number size distributions by single particle ICP-MS, J. Anal. At. Spectrom. 28 (2013) 1220–1232, https://doi.org/10.1039/c3ja50100k.

[6] F. Laborda, A.C. Gimenez-Ingalaturre, E. Bolea, J.R. Castillo, About detectability and limits of detection in single particle inductively coupled plasma mass spectrometry, Spectrochim. Acta Part B At. Spectrosc. 169 (2020), 105883, https://doi.org/10.1016/j.sab.2020.105883.

[7] P.E. Peyneau, Poisson process modelling of spike occurrence in single particle inductively coupled plasma mass spectrometry time scans for very dilute nanoparticle dispersions, Spectrochim, Acta - Part B At. Spectrosc. 178 (2021), 106126, https://doi.org/10.1016/j.sab.2021.106126.

[8] P.-E. Peyneau, M. Guillon, Number of spikes in single particle ICP-MS time scans: from the very dilute to the highly concentrated range, J. Anal. At. Spectrom. 36 (2021) 2460–2466, https://doi.org/10.1039/D1JA00156F.

[9] F. Laborda, E. Bolea, J. Jiménez-Lamana, Single particle inductively coupled plasma mass spectrometry: a powerful tool for nanoanalysis, Anal. Chem. 86 (2014) 2270–2278, https://doi.org/10.1021/ac402980q.

[10] M.D. Montaño, J.W. Olesik, A.G. Barber, K. Challis, J.F. Ranville, Single particle ICP-MS: advances toward routine analysis of nanomaterials, Anal. Bioanal. Chem. 408 (2016) 5053–5074, https://doi.org/10.1007/s00216-016-9676-8.

[11] F. Laborda, E. Bolea, J. Jiménez-Lamana, Single particle inductively coupled plasma mass spectrometry for the analysis of inorganic engineered nanoparticles in environmental samples, Trends Environ. Anal. Chem. 9 (2016) 15–23, https://doi.org/10.1016/j.teac.2016.02.001.

[12] D. Mozhayeva, C. Engelhard, A critical review of single particle inductively coupled plasma mass spectrometry – a step towards an ideal method for nanomaterial characterization, J. Anal. At. Spectrom. 35 (2020) 1740–1783, https://doi.org/10.1039/C9JA00206E.

[13] E. Bolea, M.S. Jimenez, J. Perez-Arantegui, J.C. Vidal, M. Bakir, K. Ben-Jeddou, A. C. Gimenez-Ingalaturre, D. Ojeda, C. Trujillo, F. Laborda, Analytical applications of single particle inductively coupled plasma mass spectrometry: a comprehensive and critical review, Anal. Methods 13 (2021) 2742–2795, https://doi.org/10.1039/d1ay00761k.

[14] M. Resano, M. Aramendía, E. García-Ruiz, A. Bazo, E. Bolea-Fernandez, F. Vanhaecke, Living in a transient world: ICP-MS reinvented via time-resolved analysis for monitoring single events, Chem. Sci. 13 (2022) 4436–4473, https://doi.org/10.1039/D1SC05452J.

[15] D.D. Smith, R.F. Browner, Measurement of aerosol transport efficiency in atomic spectrometry, Anal. Chem. 54 (1982) 533–537, https://doi.org/10.1021/ac00240a041.

[16] H.E. Pace, N.J. Rogers, C. Jarolimek, V.A. Coleman, C.P. Higgins, J.F. Ranville, Determining transport efficiency for the purpose of counting and sizing nanoparticles via single particle inductively coupled plasma mass spectrometry, Anal. Chem. 83 (2011) 9361–9369, https://doi.org/10.1021/ac201952t.

[17] S. Cuello-Nuñez, I. Abad-Álvaro, D. Bartczak, M.E. del Castillo Busto, D. A. Ramsay, F. Pellegrino, H. Goenaga-Infante, The accurate determination of number concentration of inorganic nanoparticles using spICP-MS with the dynamic mass flow approach, J. Anal. At. Spectrom. 35 (2020) 1832–1839, https://doi.org/10.1039/C9JA00415G.

[18] O. Geiss, I. Bianchi, G. Bucher, E. Verleysen, F. Brassinne, J. Mast, K. Loeschner, L. Givelet, F. Cubadda, F. Ferraris, A. Raggi, F. Iacoponi, R. Peters, A. Undas, A. Müller, A. Meinhardt, B. Hetzer, V. Gräf, A.R. Montoro Bustos, J. Barrero-Moreno, Determination of the transport efficiency in spICP-MS analysis using conventional sample introduction systems: an Interlaboratory comparison study, Nanomaterials 12 (2022) 725, https://doi.org/10.3390/nano12040725.

[19] LGC, Statement of measurement. Colloidal gold nanoparticles – nominal diameter 30 nm Quality Control Material LGCQC5050, 2021.

[20] J.W. Olesik, Investigating the fate of individual sample droplets in inductively coupled plasmas, Appl. Spectrosc. 51 (1997) 158A–175A, https://doi.org/10.1366/0003702971940792.

[21] C.C. Garcia, A. Murtazin, S. Groh, V. Horvatic, K. Niemax, Characterization of single Au and SiO2 nano- and microparticles by ICP-OES using monodisperse droplets of standard solutions for calibration, J. Anal. At. Spectrom. 25 (2010) 645–653, https://doi.org/10.1039/b921041e.

[22] A. Murtazin, S. Groh, K. Niemax, Measurement of element mass distributions in particle ensembles applying ICP-OES, J. Anal. At. Spectrom. 25 (2010) 1395–1401, https://doi.org/10.1039/c004946h.

[23] S. Gschwind, L. Flamigni, J. Koch, O. Borovinskaya, S. Groh, K. Niemax, D. Günther, Capabilities of inductively coupled plasma mass spectrometry for the detection of nanoparticles carried by monodisperse microdroplets, J. Anal. At. Spectrom. (2011) 1166–1174, https://doi.org/10.1039/c0ja00249f.

[24] K. Shigeta, H. Traub, U. Panne, A. Okino, L. Rottmann, N. Jakubowski, Application of a micro-droplet generator for an ICP-sector field mass spectrometer – optimization and analytical characterization, J. Anal. At. Spectrom. 28 (2013) 646–656, https://doi.org/10.1039/c2ja30207a.

[25] J. Kocic, D. Günther, B. Hattendorf, Improving detection capability for single particle inductively coupled plasma mass spectrometry with microdroplet sample introduction, J. Anal. At. Spectrom. 36 (2021) 233–242, https://doi.org/10.1039/d0ja00421a.

[26] S. Gschwind, M.D.L. Aja Montes, D. Günther, Comparison of sp-ICP-MS and MDG-ICP-MS for the determination of particle number concentration, Anal. Bioanal. Chem. (2015) 4035–4044, https://doi.org/10.1007/s00216-015-8620-7.

[27] O. Borovinskaya, B. Hattendorf, M. Tanner, S. Gschwind, D. Günther, A prototype of a new inductively coupled plasma time-of-flight mass spectrometer providing temporally resolved, multi-element detection of short signals generated by single particles and droplets, J. Anal. At. Spectrom. 28 (2013) 226–233, https://doi.org/10.1039/c2ja30227f.

[28] O. Borovinskaya, S. Gschwind, B. Hattendorf, M. Tanner, D. Günther, Simultaneous mass quantification of nanoparticles of different composition in a mixture by microdroplet generator-ICPTOFMS, Anal. Chem. 86 (2014) 8142–8148, https://doi.org/10.1021/ac501150c.

[29] L. Hendriks, B. Ramkorun-Schmidt, A. Gundlach-Graham, J. Koch, R.N. Grass, N. Jakubowski, D. Günther, Single-particle ICP-MS with online microdroplet calibration: toward matrix independent nanoparticle sizing, J. Anal. At. Spectrom. (2019) 716–728, https://doi.org/10.1039/c8ja00397a.

[30] A. Gundlach-Graham, K. Mehrabi, Monodisperse microdroplets: a tool that advances single-particle ICP-MS measurements, J. Anal. At. Spectrom. 35 (2020) 1727–1739, https://doi.org/10.1039/d0ja00213e.

[31] P. Louvat, M. Tharaud, M. Buisson, C. Rollion-Bard, M.F. Benedetti, μ-dDIHEN: a new micro-flow liquid sample introduction system for direct injection nebulization in ICP-MS, J. Anal. At. Spectrom. 34 (2019) 1553–1563, https://doi.org/10.1039/c9ja00146h.

[32] M. Tharaud, P. Louvat, M.F. Benedetti, Detection of nanoparticles by single-particle ICP-MS with complete transport efficiency through direct nebulization at few-microlitres-per-minute uptake rates, Anal. Bioanal. Chem. (2020), https://doi.org/10.1007/s00216-020-03048-y.

[33] Y. Sun, N. Liu, Y. Wang, Y. Yin, G. Qu, J. Shi, M. Song, L. Hu, B. He, G. Liu, Y. Cai, Y. Liang, G. Jiang, Monitoring AuNP dynamics in the blood of a single mouse using single particle inductively coupled plasma mass spectrometry with an ultralow-volume high-efficiency introduction system, Anal. Chem. 92 (2020) 14872–14877, https://doi.org/10.1021/acs.analchem.0c02285.

[34] S.-I. Miyashita, A.S. Groombridge, S.-I. Fujii, A. Minoda, A. Takatsu, A. Hioki, K. Chiba, K. Inagaki, Highly efficient single-cell analysis of microbial cells by time-resolved inductively coupled plasma mass spectrometry, J. Anal. At. Spectrom. 29 (2014) 1598–1606, https://doi.org/10.1039/c4ja00040d.

[35] S. Miyashita, H. Mitsuhashi, S. Fujii, A. Takatsu, K. Inagaki, T. Fujimoto, High transport efficiency of nanoparticles through a total-consumption sample introduction system and its beneficial application for particle size evaluation in single-particle ICP-MS, Anal. Bioanal. Chem. 409 (2017) 1531–1545, https://doi.org/10.1007/s00216-016-0089-5.

[36] F.H. Lin, S.I. Miyashita, K. Inagaki, Y.H. Liu, I.H. Hsu, Evaluation of three different sample introduction systems for single-particle inductively coupled plasma mass spectrometry (spICP-MS) applications, J. Anal. At. Spectrom. 34 (2019) 401–406, https://doi.org/10.1039/c8ja00295a.

[37] I. Abad-Álvaro, E. Peña-Vázquez, E. Bolea, P. Bermejo-Barrera, J.R. Castillo, F. Laborda, Evaluation of number concentration quantification by single-particle inductively coupled plasma mass spectrometry: microsecond vs. millisecond dwell times, Anal. Bioanal. Chem. 408 (2016), https://doi.org/10.1007/s00216-016-9515-y.

[38] B. Raeymaekers, T. Graule, J.A. Broekaert, F. Adams, P. Tschöpel, Characteristics of nebulized suspensions of refractory oxide powders used for the production of ceramics and their evaporation behaviour in an inductively coupled plasma, Spectrochim. Acta Part B. At. Spectrosc. 43 (1988) 923–940, https://doi.org/10.1016/0584-8547(88)80198-8.
[39] P. Goodall, M.E. Foulkes, L. Ebdon, Slurry nebulization inductively coupled plasma spectrometry-The fundamental parameters discussed, Spectrochim. Acta, Part B. 48 (1993) 1563–1577.
[40] F. Laborda, C. Trujillo, R. Lobinski, Analysis of microplastics in consumer products by single particle-inductively coupled plasma mass spectrometry using the carbon-13 isotope, Talanta. 221 (2021), 121486, https://doi.org/10.1016/j.talanta.2020.121486.
[41] D. Ojeda, E. Bolea, J. Pérez-Arantegui, F. Laborda, Exploring the boundaries in the analysis of large particles by single particle inductively coupled plasma mass spectrometry: application to nanoclays, J. Anal. At. Spectrom. 37 (2022) 1501–1511, https://doi.org/10.1039/D2JA00026A.
[42] M. Corte-Rodríguez, R. Álvarez-Fernández, P. García-Cancela, M. Montes-Bayón, J. Bettmer, Single cell ICP-MS using on line sample introduction systems: current developments and remaining challenges, TrAC - Trends Anal. Chem. 132 (2020) 116042, https://doi.org/10.1016/j.trac.2020.116042.
[43] R.C. Machado, D.F. Andrade, D.V. Babos, J.P. Castro, V.C. Costa, M.A. Sperança, J.A. Garcia, R.R. Gamela, E.R. Pereira-Filho, Solid sampling: advantages and challenges for chemical element determination—a critical review, J. Anal. At. Spectrom. 35 (2020) 54–77, https://doi.org/10.1039/C9JA00306A.
[44] J. Koch, D. Günther, Review of the state-of-the-art of laser ablation inductively coupled plasma mass spectrometry, Appl. Spectrosc. 65 (2011) 155–162, https://doi.org/10.1366/11-06255.
[45] A. Donard, F. Claverie, F. Pointurier, C. Blitz Frayret, B. Svatosova, C. Pécheyran, Direct online determination of laser-induced particle size distribution by ICPMS, Anal. Chem. 89 (2017) 8791–8799, https://doi.org/10.1021/acs.analchem.7b01041.
[46] J. Tuoriniemi, T.R. Holbrook, G. Cornelis, M. Schmitt, H.-J. Stärk, S. Wagner, Measurement of number concentrations and sizes of Au nano-particles spiked into soil by laser ablation single particle ICPMS, J. Anal. At. Spectrom. 35 (2020) 1678–1686, https://doi.org/10.1039/D0JA00243G.
[47] T.R. Holbrook, D. Gallot-Duval, T. Reemtsma, S. Wagner, An investigation into LA-spICP-ToF-MS uses for in situ measurement of environmental multi-elemental nanoparticles, J. Anal. At. Spectrom. 36 (2021) 2107–2115, https://doi.org/10.1039/d1ja00112d.
[48] Q. Li, Z. Wang, J. Mo, G. Zhang, Y. Chen, C. Huang, Imaging gold nanoparticles in mouse liver by laser ablation inductively coupled plasma mass spectrometry, Sci. Rep. 7 (2017) 1–7, https://doi.org/10.1038/s41598-017-03275-x.
[49] S. Yamashita, Y. Yoshikuni, H. Obayashi, T. Suzuki, D. Green, T. Hirata, Simultaneous determination of size and position of silver and gold nanoparticles in onion cells using laser ablation-ICP-MS, Anal. Chem. 91 (2019) 4544–4551, https://doi.org/10.1021/acs.analchem.8b05632.
[50] D. Metarapi, M. Šala, K. Vogel-Mikuš, V.S. Šelih, J.T. van Elteren, Nanoparticle analysis in biomaterials using laser ablation−single particle−inductively coupled plasma mass spectrometry, Anal. Chem. 91 (2019) 6200–6205, https://doi.org/10.1021/acs.analchem.9b00853.
[51] D. Metarapi, J.T. Van Elteren, M. Šala, K. Vogel-Mikuš, I. Arčon, V.S. Šelih, M. Kolar, S.B. Hočevar, Laser ablation-single-particle-inductively coupled plasma mass spectrometry as a multimodality bioimaging tool in nano-based omics, Environ. Sci. Nano. 8 (2021) 647–656, https://doi.org/10.1039/d0en01134g.
[52] I. Benešová, K. Dlabková, F. Zelenák, T. Vaculovič, V. Kanický, J. Preisler, Direct analysis of gold nanoparticles from dried droplets using substrate-assisted laser desorption single particle-ICPMS, Anal. Chem. 88 (2016) 2576–2582, https://doi.org/10.1021/acs.analchem.5b02421.
[53] D. Metarapi, J.T. Van Elteren, M. Šala, Studying gold nanoparticle degradation during laser ablation-single particle-inductively coupled plasma mass spectrometry analysis, J. Anal. At. Spectrom. 36 (2021) 1879–1883, https://doi.org/10.1039/d1ja00150g.
[54] D. Metarapi, J.T. van Elteren, Fundamentals of single particle analysis in biomatrices by laser ablation-inductively coupled plasma mass spectrometry, J. Anal. At. Spectrom. 35 (2020) 784–793, https://doi.org/10.1039/D0JA00003E.
[55] J.W. Olesik, P.J. Gray, Considerations for measurement of individual nanoparticles or microparticles by ICP-MS: determination of the number of particles and the analyte mass in each particle, J. Anal. At. Spectrom. 27 (2012) 1143–1155, https://doi.org/10.1039/c2ja30073g.
[56] M. Aghaei, A. Bogaerts, Particle transport through an inductively coupled plasma torch: elemental droplet evaporation, J. Anal. At. Spectrom. 31 (2016) 631–641, https://doi.org/10.1039/c5ja00162e.
[57] K.-S. Ho, K.-O. Lui, K.-H. Lee, W.-T. Chan, Considerations of particle vaporization and analyte diffusion in single-particle inductively coupled plasma-mass spectrometry, Spectrochim. Acta - Part B At. Spectrosc. 89 (2013) 30–39, https://doi.org/10.1016/j.sab.2013.08.012.
[58] J. Fuchs, M. Aghaei, T.D. Schachel, M. Sperling, A. Bogaerts, U. Karst, Impact of the particle diameter on ion cloud formation from gold nanoparticles in ICPMS, Anal. Chem. 90 (2018) 10271–10278, https://doi.org/10.1021/acs.analchem.8b02007.
[59] W.-W. Lee, W.-T. Chan, Calibration of single-particle inductively coupled plasma-mass spectrometry (SP-ICP-MS), J. Anal. At. Spectrom. 30 (2015) 1245–1254, https://doi.org/10.1039/C4JA00408F.
[60] O. Borovinskaya, M. Aghaei, L. Flamigni, B. Hattendorf, M. Tanner, A. Bogaerts, D. Günther, Diffusion- and velocity-driven spatial separation of analytes from single droplets entering an ICP off-axis, J. Anal. At. Spectrom. 29 (2014) 262–271, https://doi.org/10.1039/c3ja50307k.
[61] V. Geertsen, E. Barruet, F. Gobeaux, J.-L. Lacour, O. Taché, Contribution to accurate spherical gold nanoparticle size determination by single-particle inductively coupled mass spectrometry: a comparison with small-angle X-ray scattering, Anal. Chem. 90 (2018) 9742–9750, https://doi.org/10.1021/acs.analchem.8b01167.
[62] K.-S. Ho, W.-W. Lee, W.-T. Chan, Effects of ionization potential of an element and boiling point of the corresponding oxide on the sensitivity of ICP-MS, J. Anal. At. Spectrom. 30 (2015) 2066–2073, https://doi.org/10.1039/C5JA00137D.
[63] V. Kinnunen, S. Perämäki, R. Matilainen, Optimization of instrumental parameters for improving sensitivity of single particle inductively-coupled plasma mass spectrometry analysis of gold, Spectrochim. Acta - Part B At. Spectrosc. 177 (2021) 106104, https://doi.org/10.1016/j.sab.2021.106104.
[64] J. Liu, K.E. Murphy, R.I. MacCuspie, M.R. Winchester, Capabilities of single particle inductively coupled plasma mass spectrometry for the size measurement of nanoparticles: a case study on gold nanoparticles, Anal. Chem. 86 (2014) 3405–3414, https://doi.org/10.1021/ac403775a.
[65] A.R. Montoro Bustos, E.J. Petersen, A. Possolo, M.R. Winchester, Post hoc Interlaboratory comparison of single particle ICP-MS size measurements of NIST gold nanoparticle reference materials, Anal. Chem. 87 (2015) 8809–8817, https://doi.org/10.1021/acs.analchem.5b01741.
[66] S. Gschwind, H. Hagendorfer, D.A. Frick, D. Günther, Mass quantification of nanoparticles by single droplet calibration using inductively coupled plasma mass spectrometry, Anal. Chem. 85 (2013) 5875–5883, https://doi.org/10.1021/ac400608c.
[67] N. Jakubowski, L. Moens, F. Vanhaecke, Sector field mass spectrometers in ICP-MS, Spectrochim, Acta, Part B. At. Spectrosc. 53 (1998) 1739–1763, https://doi.org/10.1016/S0584-8547(98)00222-5.
[68] C. Suárez-Oubiña, P. Herbello-Hermelo, P. Bermejo-Barrera, A. Moreda-Piñeiro, Exploiting dynamic reaction cell technology for removal of spectral interferences in the assessment of Ag, Cu, Ti, and Zn by inductively coupled plasma mass spectrometry, Spectrochim. Acta - Part B At. Spectrosc. 187 (2022) 106330, https://doi.org/10.1016/j.sab.2021.106330.
[69] S.D. Tanner, V.I. Baranov, D.R. Bandura, Reaction cells and collision cells for ICP-MS: a tutorial review, Spectrochim. Acta - Part B At. Spectrosc. 57 (2002) 1361–1452, https://doi.org/10.1016/S0584-8547(02)00069-1.
[70] T.-S. Lum, K. Sze-Yin Leung, Strategies to overcome spectral interference in ICP-MS detection, J. Anal. At. Spectrom. 31 (2016) 1078–1088, https://doi.org/10.1039/C5JA00497G.
[71] E. Bolea-Fernandez, L. Balcaen, M. Resano, F. Vanhaecke, Overcoming spectral overlap via inductively coupled plasma-tandem mass spectrometry (ICP-MS/MS). A tutorial review, J. Anal. At. Spectrom. 32 (2017) 1660–1679, https://doi.org/10.1039/C7JA00010C.
[72] B. Bocca, E. Sabbioni, I. Mičetić, A. Alimonti, F. Petrucci, Size and metal composition characterization of nano- and microparticles in tattoo inks by a combination of analytical techniques, J. Anal. At. Spectrom. 32 (2017) 616–628, https://doi.org/10.1039/c6ja00210b.
[73] J. Nelson, A. Saunders, L. Poirier, E. Rogel, C. Ovalles, T. Rea, F. Lopez-Linares, Detection of iron oxide nanoparticles in petroleum hydrocarbon media by single-particle inductively coupled plasma mass spectrometry (spICP-MS), J. Nanopart. Res. 22 (2020) 304, https://doi.org/10.1007/s11051-020-05033-z.
[74] B. Bocca, S. Caimi, O. Senofonte, A. Alimonti, F. Petrucci, ICP-MS based methods to characterize nanoparticles of TiO2 and ZnO in sunscreens with focus on regulatory and safety issues, Sci. Total Environ. 630 (2018) 922–930, https://doi.org/10.1016/j.scitotenv.2018.02.166.
[75] J. Vidmar, L. Hässmann, K. Loeschner, Single-particle ICP-MS as a screening technique for the presence of potential inorganic nanoparticles in food, J. Agric. Food Chem. 69 (2021) 9979–9990, https://doi.org/10.1021/acs.jafc.0c07363.
[76] I. Kálomista, A. Kéri, G. Galbács, On the applicability and performance of the single particle ICP-MS nano-dispersion characterization method in cases complicated by spectral interferences, J. Anal. At. Spectrom. 31 (2016) 1112–1122, https://doi.org/10.1039/c5ja00501a.
[77] E. Bolea-Fernandez, D. Leite, A. Rua-Ibarz, L. Balcaen, M. Aramendía, M. Resano, F. Vanhaecke, Characterization of SiO2 nanoparticles by single particle-inductively coupled plasma-tandem mass spectrometry (SP-ICP-MS/MS), J. Anal. At. Spectrom. 32 (2017) 2140–2152, https://doi.org/10.1039/c7ja00138j.
[78] S. Candás-Zapico, D.J. Kutscher, M. Montes-Bayón, J. Bettmer, Single particle analysis of TiO2 in candy products using triple quadrupole ICP-MS, Talanta. 180 (2018) 309–315, https://doi.org/10.1016/j.talanta.2017.12.041.
[79] J. Wojcieszek, J. Jiménez-Lamana, L. Ruzik, M. Asztemborska, M. Jarosz, J. Szpunar, Characterization of TiO2 NPs in radish (Raphanus sativus L.) by single-particle ICP-QQQ-MS, Front. Environ. Sci. 8 (2020) 1–12, https://doi.org/10.3389/fenvs.2020.00100.
[80] J. Vidmar, P. Oprčkal, R. Milačič, A. Mladenovič, J. Ščančar, Investigation of the behaviour of zero-valent iron nanoparticles and their interactions with Cd2+ in wastewater by single particle ICP-MS, Sci. Total Environ. 634 (2018) 1259–1268, https://doi.org/10.1016/j.scitotenv.2018.04.081.
[81] J. Jiménez-Lamana, I. Abad-Álvaro, K. Bierla, F. Laborda, J. Szpunar, R. Lobinski, Detection and characterization of biogenic selenium nanoparticles in selenium-rich yeast by single particle ICPMS, J. Anal. At. Spectrom. 33 (2018) 452–460, https://doi.org/10.1039/c7ja00378a.
[82] R.J.B. Peters, A.G. Oomen, G. van Bemmel, L. van Vliet, A.K. Undas, S. Munniks, R.L.A.W. Bleys, P.C. Tromp, W. Brand, M. van der Lee, Silicon dioxide and titanium dioxide particles found in human tissues, Nanotoxicology. 14 (2020) 420–432, https://doi.org/10.1080/17435390.2020.1718232.

[83] C. Suárez-Oubiña, P. Herbello-Hermelo, P. Bermejo-Barrera, A. Moreda-Piñeiro, Single-particle inductively coupled plasma mass spectrometry using ammonia reaction gas as a reliable and free-interference determination of metallic nanoparticles, Talanta. 242 (2022) 123286, https://doi.org/10.1016/j.talanta.2022.123286.
[84] M.D. Montaño, B.J. Majestic, Å.K. Jämting, P. Westerhoff, J.F. Ranville, Methods for the detection and characterization of silica colloids by microsecond spICP-MS, Anal. Chem. 88 (2016) 4733–4741, https://doi.org/10.1021/acs.analchem.5b04924.
[85] A. Rua-Ibarz, E. Bolea-Fernandez, G. Pozo, X. Dominguez-Benetton, F. Vanhaecke, K. Tirez, Characterization of iron oxide nanoparticles by means of single-particle ICP-mass spectrometry (SP-ICP-MS)-chemical versus physical resolution to overcome spectral overlap, J. Anal. At. Spectrom. 35 (2020) 2023–2032, https://doi.org/10.1039/d0ja00183j.
[86] E. Bolea-Fernandez, D. Leite, A. Rua-Ibarz, T. Liu, G. Woods, M. Aramendia, M. Resano, F. Vanhaecke, On the effect of using collision/reaction cell (CRC) technology in single-particle ICP-mass spectrometry (SP-ICP-MS), Anal. Chim. Acta 1077 (2019) 95–106, https://doi.org/10.1016/j.aca.2019.05.077.
[87] M. Tharaud, A.P. Gondikas, M.F. Benedetti, F. Von Der Kammer, T. Hofmann, G. Cornelis, TiO2 nanomaterial detection in calcium rich matrices by spICPMS. A matter of resolution and treatment, J. Anal. At. Spectrom. 32 (2017) 1400–1411, https://doi.org/10.1039/c7ja00060j.
[88] R. Gonzalez de Vega, S. Goyen, T.E. Lockwood, P.A. Doble, E.F. Camp, D. Clases, Characterisation of microplastics and unicellular algae in seawater by targeting carbon via single particle and single cell ICP-MS, Anal. Chim. Acta 1174 (2021), 338737, https://doi.org/10.1016/j.aca.2021.338737.
[89] K.H. Chun, J.T.S. Lum, K.S.Y. Leung, Dual-elemental analysis of single particles using quadrupole-based inductively coupled plasma-mass spectrometry, Anal. Chim. Acta 1192 (2022), 339389, https://doi.org/10.1016/j.aca.2021.339389.
[90] L.A. Rush, M.C. Endres, M. Liezers, J.D. Ward, G.C. Eiden, A.M. Duffin, Collisional dampening for improved quantification in single particle inductively coupled plasma mass spectrometry, Talanta. 189 (2018) 268–273, https://doi.org/10.1016/j.talanta.2018.06.071.
[91] N.D. Donahue, S. Kanapilly, C. Stephan, M.C. Marlin, E.R. Francek, M. Haddad, J. Guthridge, S. Wilhelm, Quantifying chemical composition and reaction kinetics of individual colloidally dispersed nanoparticles, Nano Lett. 22 (2022) 294–301, https://doi.org/10.1021/acs.nanolett.1c03752.
[92] M.D. Montaño, H.R. Badiei, S. Bazargan, J.F. Ranville, Improvements in the detection and characterization of engineered nanoparticles using spICP-MS with microsecond dwell times, Environ. Sci. Nano. 1 (2014) 338, https://doi.org/10.1039/C4EN00058G.
[93] A. Hineman, C. Stephan, Effect of dwell time on single particle inductively coupled plasma mass spectrometry data acquisition quality, J. Anal. At. Spectrom. 29 (2014) 1252, https://doi.org/10.1039/c4ja00097h.
[94] S. Meyer, R.G. De Vega, X. Xu, Z. Du, P.A. Doble, D. Clases, Characterization of upconversion nanoparticles by single-particle ICP-MS employing a quadrupole mass filter with increased bandpass, Anal. Chem. 92 (2020) 15007–15016, https://doi.org/10.1021/acs.analchem.0c02925.
[95] P. Shaw, A. Donard, Nanoparticle analysis using dwell times between 10 μs and 70 μs with an upper counting limit of greater than 3×10^7 cps and a gold nanoparticle detection limit of less than 10 nm diameter, J. Anal. At. Spectrom 31 (2016) 1234–1242, https://doi.org/10.1039/c6ja00047a.
[96] J. Tuoriniemi, G. Cornelis, M. Hassellöv, Size discrimination and detection capabilities of single-particle ICPMS for environmental analysis of silver nanoparticles, Anal. Chem. 84 (2012) 3965–3972, https://doi.org/10.1021/ac203005r.
[97] Z. Li, M. Hadioui, K.J. Wilkinson, Conditions affecting the release of thorium and uranium from the tailings of a niobium mine, Environ. Pollut. 247 (2019) 206–215, https://doi.org/10.1016/j.envpol.2018.12.042.
[98] J.L. Wang, E. Alasonati, M. Tharaud, A. Gelabert, P. Fisicaro, M.F. Benedetti, Flow and fate of silver nanoparticles in small French catchments under different land-uses: the first one-year study, Water Res. 176 (2020) 115722, https://doi.org/10.1016/j.watres.2020.115722.
[99] K. Phalyvong, Y. Sivry, H. Pauwels, A. Gélabert, M. Tharaud, G. Wille, X. Bourrat, M.F. Benedetti, Occurrence and origins of cerium dioxide and titanium dioxide nanoparticles in the Loire River (France) by single particle ICP-MS and FEG-SEM imaging, Front. Environ. Sci. 8 (2020) 1–14, https://doi.org/10.3389/fenvs.2020.00141.
[100] A. Azimzada, J.M. Farner, M. Hadioui, C. Liu-Kang, I. Jreije, N. Tufenkji, K. J. Wilkinson, Release of TiO2 nanoparticles from painted surfaces in cold climates: characterization using a high sensitivity single-particle ICP-MS, Environ. Sci. Nano. 7 (2020) 139–148, https://doi.org/10.1039/c9en00951e.
[101] M. Hadioui, G. Knapp, A. Azimzada, I. Jreije, L. Frechette-Viens, K.J. Wilkinson, Lowering the size detection limits of Ag and TiO_2 nanoparticles by single particle ICP-MS, Anal. Chem. 91 (2019) 13275–13284, https://doi.org/10.1021/acs.analchem.9b04007.
[102] I. Jreije, A. Azimzada, M. Hadioui, K.J. Wilkinson, Measurement of CeO_2 nanoparticles in natural waters using a high sensitivity Single Particle ICP-MS, Molecules 25 (2020) 5516, https://doi.org/10.3390/molecules25235516.
[103] A. Gondikas, F. Von Der Kammer, R. Kaegi, O. Borovinskaya, E. Neubauer, J. Navratilova, A. Praetorius, G. Cornelis, T. Hofmann, Where is the nano? Analytical approaches for the detection and quantification of TiO2 engineered nanoparticles in surface waters, Environ. Sci. Nano. 5 (2018) 313–326, https://doi.org/10.1039/c7en00952f.
[104] A. Gundlach-Graham, Multiplexed and multi-metal single-particle characterization with ICP-TOFMS, in: J.V. Radmila Milačič, Janez Ščančar, Heidi Goenaga-Infante (Eds.), Compr. Anal. Chem, Elsevier, 2021, pp. 69–101, https://doi.org/10.1016/BS.COAC.2021.01.008.
[105] S. Naasz, S. Weigel, O. Borovinskaya, A. Serva, C. Cascio, A.K. Undas, F. C. Simeone, H.J.P. Marvin, R.J.B. Peters, Multi-element analysis of single nanoparticles by ICP-MS using quadrupole and time-of-flight technologies, J. Anal. At. Spectrom. 33 (2018) 835–845, https://doi.org/10.1039/c7ja00399d.
[106] F. Loosli, J. Wang, S. Rothenberg, M. Bizimis, C. Winkler, O. Borovinskaya, L. Flamigni, M. Baalousha, Sewage spills are a major source of titanium dioxide engineered (nano)-particle release into the environment, Environ. Sci. Nano. 6 (2019) 763–777, https://doi.org/10.1039/c8en01376d.
[107] S.E. Szakas, R. Lancaster, R. Kaegi, A. Gundlach-Graham, Quantification and classification of engineered, incidental, and natural cerium-containing particles by spICP-TOFMS, Environ. Sci. Nano. 9 (2022) 1627–1638, https://doi.org/10.1039/d1en01039e.
[108] A. Azimzada, J.M. Farner, I. Jreije, M. Hadioui, C. Liu-Kang, N. Tufenkji, P. Shaw, K.J. Wilkinson, Single- and multi-element quantification and characterization of TiO_2 nanoparticles released from outdoor stains and paints, Front. Environ. Sci. 8 (2020) 91, https://doi.org/10.3389/fenvs.2020.00091.
[109] L. Hendriks, A. Gundlach-graham, B. Hattendorf, Characterization of a new ICP-TOFMS instrument with continuous and discrete introduction of solutions †, J. Anal. At. Spectrom. 32 (2017) 548–561, https://doi.org/10.1039/c6ja00400h.
[110] A. Praetorius, A. Gundlach-Graham, E. Goldberg, W. Fabienke, J. Navratilova, A. Gondikas, R. Kaegi, D. Günther, T. Hofmann, F. Von Der Kammer, Single-particle multi-element fingerprinting (spMEF) using inductively-coupled plasma time-of-flight mass spectrometry (ICP-TOFMS) to identify engineered nanoparticles against the elevated natural background in soils, Environ. Sci. Nano. 4 (2017) 307–314, https://doi.org/10.1039/c6en00455e.
[111] A. Hegetschweiler, O. Borovinskaya, T. Staudt, T. Kraus, Single-particle mass spectrometry of titanium and niobium carbonitride precipitates in steels, Anal. Chem. 91 (2019) 943–950, https://doi.org/10.1021/acs.analchem.8b04012.
[112] K. Mehrabi, R. Kaegi, D. Günther, A. Gundlach-Graham, Automated single-nanoparticle quantification and classification: a holistic study of particles into and out of wastewater treatment plants in Switzerland, Environ. Sci. Nano. 8 (2021) 1211–1225, https://doi.org/10.1039/d0en01066a.
[113] J.S. Becker, Inorganic Mass Spectrometry: Principles and Applications, John Wiley & Sons, Ltd, Chichester, 2007.
[114] I. Strenge, C. Engelhard, Single particle inductively coupled plasma mass spectrometry: investigating nonlinear response observed in pulse counting mode and extending the linear dynamic range by compensating for dead time related count losses on a microsecond timescale, J. Anal. At. Spectrom. 35 (2020) 84–99, https://doi.org/10.1039/C9JA00327D.
[115] C. Degueldre, P. Favarger, S. Wold, Gold colloid analysis by inductively coupled plasma-mass spectrometry in a single particle mode, Anal. Chim. Acta 555 (2006) 263–268, https://doi.org/10.1016/j.aca.2005.09.021.
[116] S. Yongyang, W. Wei, L. Zhiming, D. Hu, Z. Guoqing, X. Jiang, R. Xiangjun, Direct detection and isotope analysis of individual particles in suspension by single particle mode MC-ICP-MS for nuclear safety, J. Anal. At. Spectrom. 30 (2015) 1184–1190, https://doi.org/10.1039/c4ja00339j.
[117] S. Yamashita, K. Yamamoto, H. Takahashi, T. Hirata, Size and isotopic ratio measurements of individual nanoparticles by a continuous ion-monitoring method using *f*araday detectors equipped on a multi-collector-ICP-mass spectrometer, J. Anal. At. Spectrom. 37 (2022) 178–184, https://doi.org/10.1039/d1ja00312g.
[118] I. Strenge, C. Engelhard, Capabilities of fast data acquisition with microsecond time resolution in inductively coupled plasma mass spectrometry and identification of signal artifacts from millisecond dwell times during detection of single gold nanoparticles, J. Anal. At. Spectrom. 31 (2016) 135–144, https://doi.org/10.1039/C5JA00177C.
[119] J. Tuoriniemi, G. Cornelis, M. Hassellöv, A new peak recognition algorithm for detection of ultra-small nano-particles by single particle ICP-MS using rapid time resolved data acquisition on a sector-field mass spectrometer, J. Anal. At. Spectrom. 30 (2015) 1723–1729, https://doi.org/10.1039/C5JA00113G.
[120] A.M. Duffin, E.D. Hoegg, R.I. Sumner, T. Cell, G.C. Eiden, L.S. Wood, Temporal analysis of ion arrival for particle quantification, J. Anal. At. Spectrom. 36 (2021) 133–141, https://doi.org/10.1039/d0ja00412j.
[121] L. Hendriks, A. Gundlach-Graham, D. Günther, Performance of sp-ICP-TOFMS with signal distributions fitted to a compound Poisson model, J. Anal. At. Spectrom. 34 (2019) 1900–1909, https://doi.org/10.1039/C9JA00186G.
[122] K. Newman, C. Metcalfe, J. Martin, H. Hintelmann, P. Shaw, A. Donard, Improved single particle ICP-MS characterization of silver nanoparticles at environmentally relevant concentrations, J. Anal. At. Spectrom. 31 (2016) 2069–2077, https://doi.org/10.1039/c6ja00221h.
[123] R. Peters, Z. Herrera-Rivera, A. Undas, M. van der Lee, H. Marvin, H. Bouwmeester, S. Weigel, Single particle ICP-MS combined with a data evaluation tool as a routine technique for the analysis of nanoparticles in complex matrices, J. Anal. At. Spectrom. 30 (2015) 1274–1285, https://doi.org/10.1039/C4JA00357H.
[124] T.E. Lockwood, R. Gonzalez De Vega, D. Clases, An interactive Python-based data processing platform for single particle and single cell ICP-MS, J. Anal. At. Spectrom. 36 (2021) 2536–2544, https://doi.org/10.1039/d1ja00297j.
[125] A. Felinger, G. Guiochon, Validation of a chromatography data analysis software, J. Chromatogr. A 913 (2001) 221–231, https://doi.org/10.1016/S0021-9673(00)00979-1.
[126] G. Cornelis, M. Hassellöv, A signal deconvolution method to discriminate smaller nanoparticles in single particle ICP-MS, J. Anal. At. Spectrom. 29 (2014) 134–144, https://doi.org/10.1039/c3ja50160d.

[127] G. Cornelis, S. Rauch, Drift correction of the dissolved signal in single particle ICPMS, Anal. Bioanal. Chem. 408 (2016) 5075–5087, https://doi.org/10.1007/s00216-016-9509-9.
[128] D. Mozhayeva, C. Engelhard, A quantitative nanoparticle extraction method for microsecond time resolved single-particle ICP-MS data in the presence of a high background, J. Anal. At. Spectrom. 34 (2019) 1571–1580, https://doi.org/10.1039/c9ja00042a.
[129] I. Kálomista, A. Kéri, D. Ungor, E. Csapó, I. Dékány, T. Prohaska, G. Galbács, Dimensional characterization of gold nanorods by combining millisecond and microsecond temporal resolution single particle ICP-MS measurements, J. Anal. At. Spectrom. 32 (2017) 2455–2462, https://doi.org/10.1039/c7ja00306d.
[130] E. Bolea-Fernandez, A. Rua-Ibarz, M. Velimirovic, K. Tirez, F. Vanhaecke, Detection of microplastics using inductively coupled plasma-mass spectrometry (ICP-MS) operated in single-event mode, J. Anal. At. Spectrom. 35 (2020) 455–460, https://doi.org/10.1039/C9JA00379G.
[131] L.D. Scanlan, R.B. Reed, A.V. Loguinov, P. Antczak, A. Tagmount, S. Aloni, D. T. Nowinski, P. Luong, C. Tran, N. Karunaratne, D. Pham, X.X. Lin, F. Falciani, C. P. Higgins, J.F. Ranville, C.D. Vulpe, B. Gilbert, Silver nanowire exposure results in internalization and toxicity to daphnia magna, ACS Nano 7 (2013) 10681–10694, https://doi.org/10.1021/nn4034103.
[132] Y. Echegoyen, S. Rodríguez, C. Nerín, Nanoclay migration from food packaging materials, Food Addit. Contam. Part A. 33 (2016) 530–539, https://doi.org/10.1080/19440049.2015.1136844.
[133] R.B. Reed, D.G. Goodwin, K.L. Marsh, S.S. Capracotta, C.P. Higgins, D. H. Fairbrother, J.F. Ranville, Detection of single walled carbon nanotubes by monitoring embedded metals, Environ Sci Process Impacts 15 (2013) 204–213, https://doi.org/10.1039/C2EM30717K.
[134] J. Wang, R.S. Lankone, R.B. Reed, D.H. Fairbrother, J.F. Ranville, Analysis of single-walled carbon nanotubes using spICP-MS with microsecond dwell time, NanoImpact. 1 (2016) 65–72, https://doi.org/10.1016/j.impact.2016.04.004.
[135] R.S. Lankone, J. Wang, J.F. Ranville, D.H. Fairbrother, Photodegradation of polymer-CNT nanocomposites: effect of CNT loading and CNT release characteristics, Environ. Sci. Nano. 4 (2017) 967–982, https://doi.org/10.1039/c6en00669h.
[136] T. Vonderach, B. Hattendorf, D. Günther, New orientation: a downward-pointing vertical inductively coupled plasma mass spectrometer for the analysis of microsamples, Anal. Chem. 93 (2021) 1001–1008, https://doi.org/10.1021/acs.analchem.0c03831.
[137] T. Vonderach, D. Gunther, Fundamental studies on droplet throughput and the analysis of single cells using a downward-pointing ICP-time-of-flight mass spectrometer, J. Anal. At. Spectrom. 36 (2021) 2617–2630, https://doi.org/10.1039/d1ja00243k.